Fire Technology

Extinguishing smoldering fires in wood pellets with water cooling- an experimental study

--Manuscript Draft--

Manuscript Number:	FIRE-D-18-00171R1
Full Title:	Extinguishing smoldering fires in wood pellets with water cooling- an experimental study
Article Type:	Manuscript
Keywords:	fuel storage; industrial fire; biofuels; smoldering; extinguishment; fire suppression; spontaneous combustion; self-heating; biomass, storage safety
Corresponding Author:	Ragni Fjellgaard Mikalsen RISE Fire Research Trondheim, NORWAY
Corresponding Author Secondary Information:	
Corresponding Author's Institution:	RISE Fire Research
Corresponding Author's Secondary Institution:	
First Author:	Ragni Fjellgaard Mikalsen
First Author Secondary Information:	
Order of Authors:	Ragni Fjellgaard Mikalsen
	Bjarne Christian Hagen
	Anne Steen-Hansen
	Ulrich Krause
	Vidar Frette
Order of Authors Secondary Information:	
Funding Information:	Norges Forskningsråd (238329) — Dr Vidar Frette
Abstract:	Smoldering fires in stored or transported solid biofuels are very difficult to extinguish. The current study has explored heat extraction from the combustion zone as a method for extinguishing such flameless fires. Heat extraction from the sample was made feasible using water flowing through a metal pipe located inside the sample. The fuel container was a steel cylinder with insulated side walls, open at the top and heated from below. Wood pellets (1.25 kg, 1.8 liters) was used as fuel. Results from small-scale experiments provide proof-of-concept of cooling as a new extinguishing method for smoldering fires. During self-sustained smoldering with heat production in the range 0-60 W, the heat loss to the cooling unit was in the range 5-20 W. There were only marginal differences between non-extinguished and extinguished cases. Up-scaling is discussed, cooling could be feasible for preventing smoldering fires in silos.

Fire Technology manuscript No.
(will be inserted by the editor)

Extinguishing smoldering fires in wood pellets with water cooling- an experimental study

First Author · Second Author

Received: date / Accepted: date

Abstract Smoldering fires in stored or transported solid biofuels are very difficult to extinguish. The current study has explored heat extraction from the combustion zone as a method for extinguishing such flameless fires. Heat extraction from the sample was made feasible using water flowing through a metal pipe located inside the sample. The fuel container was a steel cylinder with insulated side walls, open at the top and heated from below. Wood pellets (1.25 kg, 1.8 liters) was used as fuel. Results from small-scale experiments provide proof-of-concept of cooling as a new extinguishing method for smoldering fires. During self-sustained smoldering with heat production in the range 0-60 W, the heat loss to the cooling unit was in the range 5-20 W. There were only marginal differences between non-extinguished and extinguished cases. Up-scaling is discussed, cooling could be feasible for preventing smoldering fires in silos.

Keywords Fuel storage safety · Industrial fire · Biofuels · Smoldering · Extinguishment · Fire suppression

1 Introduction

Smoldering fires are regularly observed in industrial facilities such as biofuel silos, flat storage units, cargo vessels and waste deposits [1]. This flameless form of fire causes problems in large deposits, due to self-heating of the biomass [2]. Smoldering in silos and deposits might be perceived as less harmful than flaming fires, but smoldering can inflict severe damage. A smoldering fire will consume products in a storage unit, while emitting toxic smoke that may be harmful to people in nearby domestic areas as well as for workers at the facility.

As smoldering propagates through a material, heat is produced through heterogeneous reactions between air and the solid surface [3]. The heat from the combustion promotes pyrolysis and the formation of pyrolyzate gases. These are not consumed in the smoldering process, but may ignite outside the smoldering zone and give flaming fire or explosion given a sufficiently high gas volume and

Address(es) of author(s) should be given

concentration. The conditions leading to such transitions are not easily predicted. [3,4]

Industrially, it has proven challenging for fire brigades to detect, control and extinguish smoldering fires. There are essentially no guaranteed and cost-effective extinguishing procedures for large-scale industrial storage units [2].

A commonly used method to control and extinguish smoldering fires is to remove the fuel from the storage unit, and drench it with water [2,5]. This fire-fighting method may result in production stop and in destruction of the product. For some storage units such as silos, forced manual opening of the storage unit may be necessary. For flat storage units, or outdoor storages like landfills, the enormous scale of the fuel bed often makes a complete extinguishment by fuel removal impossible. The fire-fighting strategy often has to be adjusted, from aiming at extinguishment to instead controlling the fire [6,7]. Fuel removal during smoldering will often require personnel present at or near the combustion site, causing a risk of injury due to asphyxiation, toxic gases, or explosion [2,5].

Removing the fuel is one way of extinguishing a smoldering fire, two other options are to quench the oxygen supply to the reaction zone through inertisation or to cool the reaction zone.

Inertisation has been used both at full-scale and in laboratory-scale experiments, either to control the combustion until other measures may be taken, or to completely quench the fire. Industrially, carbon dioxide (CO_2) and nitrogen gas (N_2) are most commonly used due to availability and cost [5]. In silos, CO_2 is best applied from the top since its density is larger than that of air, while N_2 may be applied from both the top and the bottom, with easier access [5,8]. Regardless of gas choice, if the gaseous suppression system is not pre-installed in the industrial storage unit, penetration of the gas into the fuel bed may be insufficient for complete extinguishment. Holding times of the gas extinguishing efforts for complete quenching of smoldering is very long compared with flaming (days or months vs minutes or hours) [9], and re-ignition is common both at industrial and laboratory-scale [2,8,10,11]. For all inert-gas systems, suffocation and toxic effects for humans present in the facility represent hazards. Also, rapid injection of gases may cause dust clouds, which may lead to dust explosions [5].

For the third option, cooling the reaction zone, water is the most widely used cooling agent. However, water in large fuel beds will find the path of least flow resistance. The subsequent channeling gives an uneven distribution of the water, which will not necessarily reach the combustion zone [3]. At laboratory-scale, the amount of water needed for extinguishment is in the range of 1-6 liters of water per kilogram fuel [3,10]. Industrially, the additional weight of the water may damage the structural integrity of the storage unit. Rupture of the storage unit may also be caused by swelling of compressed fuels, such as pellets, when in contact with water [2,5]. To limit the amount of water, sprays [9] and water mists [11] have been used at laboratory-scale, with limited success. Water sprays, mists and showers may even cause scattering of glowing embers or dust dispersion to hazardous dust clouds [5]. Foams may be used to increase the wetting of the fuel, but this is still not an effective extinguishing method [8], often foams are used only as an explosion prevention measure applied to the top of the biomass [2]. At large-scale, water and foam runoff to nearby rivers and lakes may be harmful to the environment [12,13].

Cooling the fuel bed without direct contact between water and fuel can be a way to avoid channeling, swelling, scattering and water runoff. This approach

is currently being tested at large-scale in St. Louis, USA, where an underground smoldering fire in a landfill is approaching nuclear waste. Cooling liquid is pumped through pipes sunken into the ground to absorb heat [6,7]. The outcome of this case study has not been published yet. A numerical study of a similar system showed that the spacial extent of the cooling was limited, suggesting that local cooling around a cooling pipe would have a very limited impact on a smoldering fire[1].

This article presents the first experimental study on such a system, in which cooling of smoldering is obtained without direct contact between water and fuel. A heat exchanger in the form of a metal pipe with water flow is inserted into the fuel bed and used to extract heat. The potential for prevention, control or extinguishment of smoldering is explored. The study is based on laboratory-scale experiments with wood pellets as fuel. Application and up-scaling to industrial-scale is discussed.

2 Material and methods

2.1 Wood pellet fuel

The pellets were produced in Norway and consisted of 20-50 % pine and 50-80 % spruce, including bark. Pellets with pine/spruce mixture have been shown to be reactive and prone to self-heating [14]. Pellet diameter was 8.2 ± 0.2 mm (range 7.5-8.9 mm), pellet length 13.5 ± 6 mm (range 2.8-34.3 mm), mass of each pellet 0.8 ± 0.4 g (range 0.04-2.0 g), the distribution of these properties is given in Fig. 1.

The chemical composition of the pellets as received was 48 % carbon, 39 % oxygen, 6 % hydrogen, 0 % nitrogen, measured by Leco CHN 1000 and Leco CS230 elemental analyzers. Proximate analysis of the sample as received, gave a content of 6.3 % moisture, 77 % volatiles, 0.46 % ash, measured by Leco 701 thermogravimetric analyzer.

The activation energy of the pellets was 91.4 kJ/mol determined by adiabatic testing [15]. The total heat of combustion was 17.4 MJ/kg without water and 18.8 MJ/kg with water (aka. the upper and lower calorific values), measured by IKA C200 bomb calorimeter.

The heat conductivity was in the range 0.15-0.25 W/mK, measured for ground wood pellets by hot disc method (not suitable for measurement of whole pellets). The bulk permeability was below $2.4 \cdot 10^{-8}$ m^2, as measured using a self-built flow device. The bulk density as used in the experiments was approximately 710 kg/m^3.

The pellets were sampled by the producer 3 months after production. The received pellets consisted mainly of whole pellets, with < 1 wt% fine particles (< 4 mm x 4 mm). The pellets were stored in closed 10 kg bags at -25 °C, to ensure that the reactivity of the pellets remained unchanged for all experiments in a series, as recommended by Larsson et al [16]. The pellets were taken from the freezer 1-2 days prior to the experiment, and defrosted at ambient temperature (22 ± 1 °C).

[1] Access to the unpublished report "Numerische Modellierung der Brandausbreitung infolge Selbstentzndung ohne und mit Heatpipes", by H.Krause, 2010, was granted by Prof. U.Krause at OvG University Magdeburg, Germany.

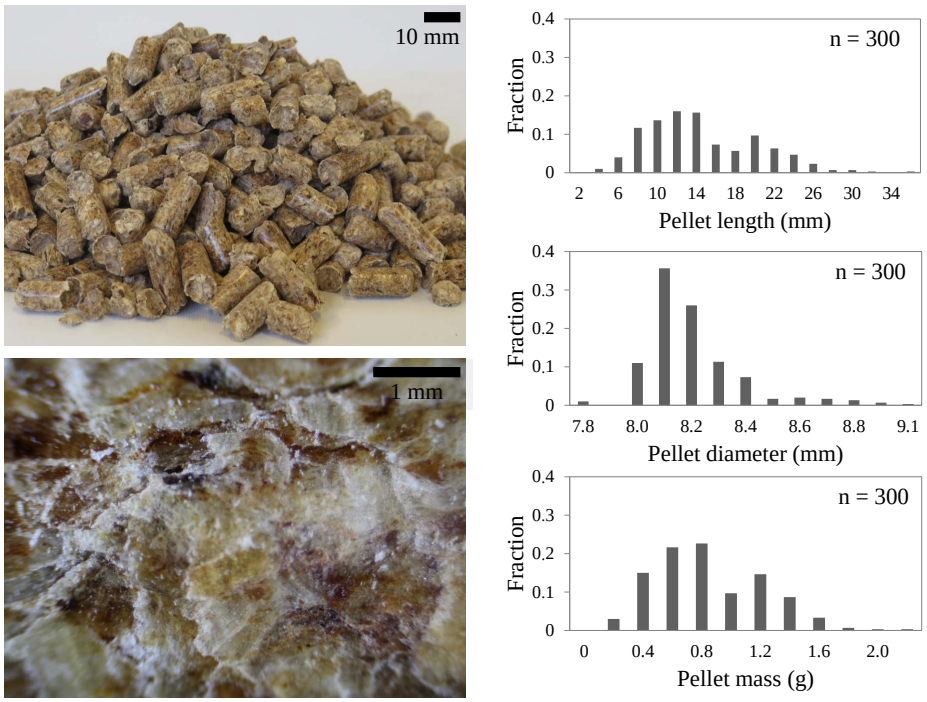

Figure 1 Photos of wood pellets fuel (left). The top photo (10 mm scale bar) shows its granular nature. The bottom photo (1 mm scale bar) shows that each pellet is inhomogeneous, consisting of compacted wood dusts of varying content (high bark content is seen as dark areas). Distributions of length, diameter and mass of the pellets are given (right).

2.2 Experimental set-up

The experimental set-up is shown in Fig. 2. The experimental set-up has been developed within the research project EMRIS, and has previously been used for experiments with smoldering in biomaterials [17,18]. A Kern 30 kg IP65 weighing platform connected to a Systech IT 1000 4-20 MAMP digital scale, with a precision of 1 g was placed on a horizontal surface. A Wilfa CP1 electrical heating unit of 2000 W was placed on top of the scale. The top of the electrical heating unit consisted of an 185 mm diameter ceramic disc, onto which a fitted aluminum plate was placed. The aluminum plate was 280 mm x 280 mm x 30 mm and distributed heat evenly to the lower part of the sample. On top of the aluminum plate a stainless-steel cylinder was placed. The cylinder diameter was 150 mm, wall thickness 1 mm. The side walls of the cylinder were insulated by 60 mm mineral wool with thermal conductivity 0.041 W/mK at 50 °C, 0.085 W/mK at 300 °C. The top end of the stainless-steel cylinder was not insulated, and vertical heat conduction could occur. The cylinder thereby makes up a side-insulated sample container that was open to air convection at the top and closed at the bottom.

Encapsulated 0.5 mm K-type thermocouples were used to monitor temperatures in the sample. One thermocouple was placed in a slit at the top of the aluminum plate, measuring its top, center temperature, hereby denoted as the

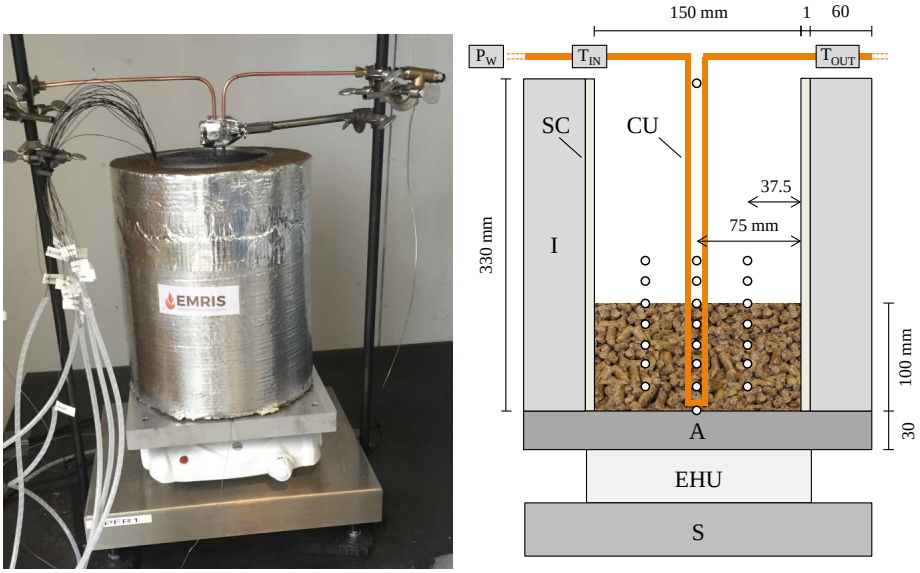

Figure 2 Photo and sketch of the set-up. Scale (S), electric heating unit (EHU), aluminum plate (A), insulation (I), steel cylinder (SC), cooling unit (CU), water pressure (Pw) and water temperature measurement positions (T_{IN}, T_{OUT}). Thermocouple positions in the sample container are marked by (o). The sketch is not to scale, dimensions are given in mm.

"heater" position. Above the heater, thermocouples were positioned at heights from 20 mm to 140 mm, three at each level - one in the center, and two equidistant between center and steel pipe (at 37.5 mm from the center), see Fig. 2 -right. In addition, one thermocouple was placed in the center, 330 mm above the heater. . The thermocouples were attached to a small stainless-steel structure shaped like a ladder, to maintain their designated location throughout the experiments. The structure was rigid in the vertical direction, but the horizontal position could vary ($\pm$ 10 mm) due to the thin steel bands it consisted of.

Experiments were performed with and without cooling of the fuel bed, see details in section 2.5. For the experiments without cooling, the equipment described above was the complete experimental set-up. For experiments with cooling of the fuel bed, a cooling unit was used.

The cooling unit consisted of a 4.76 mm outer diameter copper pipe, bent into a U-shape (see Fig. 2 and 3b) with inner separation between the two tube branches of about 15 mm and outer distance about 24 mm (Fig. 3e). The U-shaped pipe was inserted into the cylinder, near the center, in such a way that it was not in contact with the thermocouple ladder. The lower tip of the pipe was positioned 10 mm above the heater, to avoid conductive heat transfer between the two (Fig. 3d). The total volume of the cooling unit located within the sample was $4.5{\cdot}10^{-6}$ m^3 (0.0045 liters), corresponding to 0.3 vol% of the sample volume of 0.0018 m^3 (1.8 liters). The inlet and outlet of the copper pipe were supported by a rack. The water outlet was connected to tubes leading to a drain. The water inlet was connected to the municipal water supply, with some variations in the water pressure and temperature. The water temperature was 16 $\pm$ 2 °C. The water temperatures

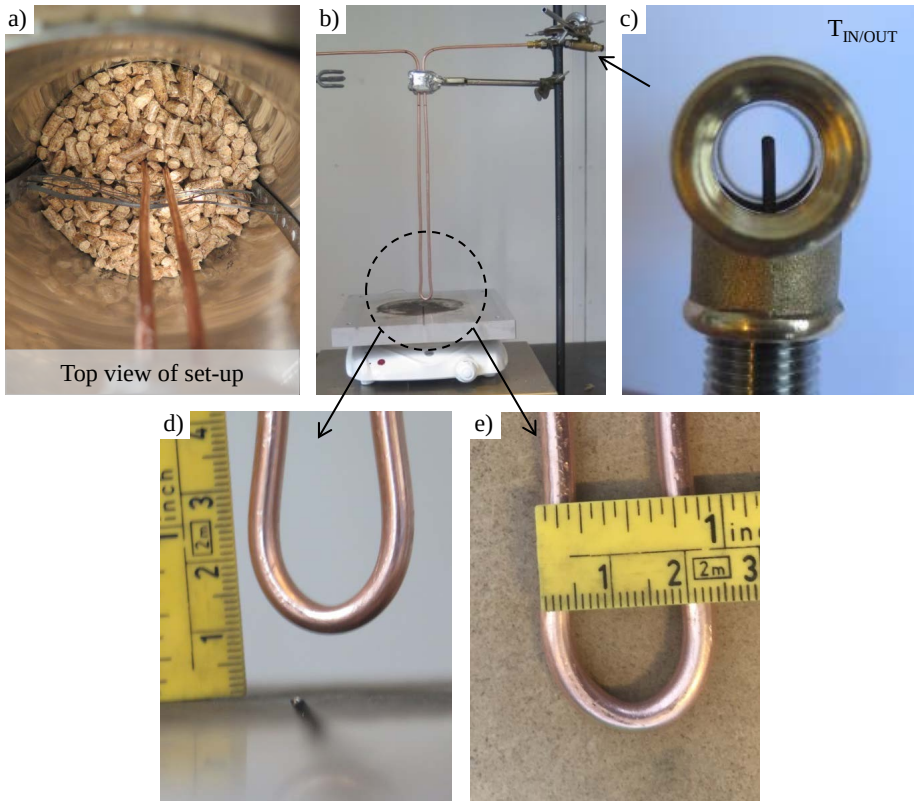

Figure 3 Detail photos of set-up. (a) Top view of set-up, with central location of the cooling unit, the position of the thermocouple ladder and the relative size of the cooling unit compared with the fuel bed diameter. (b) Cooling unit without surrounding steel cylinder. (c) Cross section of cooling pipe, thermocouples measuring water temperatures (T_{IN} and T_{OUT}) were located near its center. (d) Separation between cooling unit and aluminum plate. (e) Separation between the two tube branches of the cooling unit.

were measured at the inlet and at the outlet of the cooling unit, near the top of the cylinder, as shown in Fig. 2-right. Water temperatures were measured by 1.5 mm encapsulated type K thermocouples near the center of the cooling pipe (Fig. 3c).

The inlet water pressure was regulated to 0.57 bar, giving a water flow rate during experiments around 0.63 L/min (see Table 2 for scenario specific details). Water pressure of the water inlet was measured using a 0-25 bar Keller piezoresistive pressure transmitter PA-23SY, positioned about 2 meters from the experimental set-up.

Data was recorded at intervals of 5 seconds. The experimental set-up was placed inside a ventilation hood, with a constant low air extraction. The experimental period was June 2016 - May 2017. The ambient temperature in the room was 21.7 $\pm$ 1.0 °C.

2.3 Experimental procedure

The experimental set-up was assembled as described in section 2.2. The defrosted pellets (1.25 kg, 1.8 liters) were poured into the cylinder using a small cup. This amount of pellets gives a sample height of approximately 100 mm, which was chosen based on previous experiments [19]: Lower sample heights were not used to optimize reproducibility and limit susceptibility to sampling. Higher sample heights were not used to limit the total time from start till burn-out to a few days.

For the experiments with cooling, the water flow through the cooling unit was started at a specific time for each scenario. Details on cooling scenarios are given in section 2.5 and Table 1.

The heating procedure was based on preliminary experiments. Data logging was started 2 minutes prior to the external heater was switched on. External heating was started by setting the power of the electrical heating unit to its maximum value of 2000 W. Temperatures increased until a set-point temperature of 370 °C was obtained between the electric heating unit and the aluminum plate, which took about 1 h. After this, a regulator was used to maintain the set-point temperature by switching the electrical heating unit on and off, giving an average power input of approximately 860 W. The temperature at the top of the aluminum plate was lower than the set-point temperature due to heat loss through the aluminum plate. After the initial temperature increase period, and through the remaining external heating period, the temperature at the top of the aluminum plate, which was in contact with the fuel, was 348 ± 7 °C. The heat loss through the aluminum plate could have been reduced through the use of thermal insulation. However, this would not have allowed rapid cooling of the aluminum plate after the electrical heating unit was switched off. With thermal insulation, the aluminum plate would have functioned as a thermal reservoir, which could have affected the smoldering. The duration of the external heating period was chosen based on preliminary experiments to ensure that a self-sustained smoldering was obtained, see Table 1. Self-sustained smoldering is defined here as increasing temperatures within the sample after the external heating was switched off.

After the external heating was switched off, the system was left undisturbed until the end of the experiment. The experiment was considered finished when all sample temperatures had decreased below 30 °C, with a decreasing trend. Data was recorded for at least 1 h after this.

After the end of each experiment, the sample residue was removed from the experimental set-up and sorted based on physical appearance: original pellets, semi-brown pellets, brown pellets, black pellets, wood dusts (< 4 mm x 4 mm) and ash (< 4 mm x 4 mm). Ash and wood dusts were not observed in the same residue for any of the experiments. In addition to the expected discoloration due to combustion, some of the pellets in direct contact with the copper cooling pipe were partially green in color, indicating oxidation of the copper. However, there was no visible deterioration of the copper cooling unit, the same unit was used for all cooling experiments. After each experiment, the stainless-steel cylinder, aluminum plate and cooling pipe were cleaned, removing tar and other residue sticking to the equipment. This procedure also included draining the cooling pipe of water before the next experiment.

The height of the sample was measured with a ruler before and after each experiment (precision around ±10 mm). These start- and end-heights are given

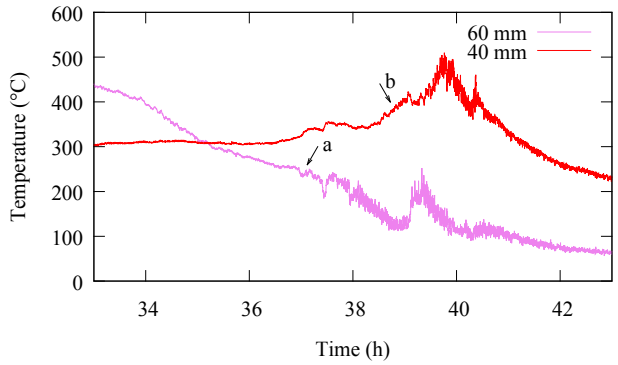

Figure 4 Example of sample height estimation: Temperatures as a function of time are given for two thermocouple locations. At time *a*, the temperature recording located at 60 mm height displays increased fluctuations. At this time, the estimated minimum sample height is reduced by 20 mm, from 60 mm to 40 mm, see details in main text. The same applies for *b* at 40 mm. Data every 5 seconds is shown. The full experiment is given under scenario C in Fig. 6.

by lines in Fig. 6-bottom. After an experiment, the top surface was uneven, and the end-height is therefore given by three lines, representing the measured minimum, average and maximum heights. In the time span between these manual measurements, temperature readings were used to estimate sample height. Thin thermocouples are sensitive to convection [20]. The thin 0.5 mm thermocouples used in this study therefore displayed higher fluctuation for thermocouples located near, or in free air, compared with thermocouples located within the sample. Each thermocouple thereby provides a time estimate for when the top of the sample had reached or passed that thermocouple position (see Fig. 4). Each such time estimate is shown by a cross in Fig. 6-bottom. There were three thermocouples at each level, with 37.5 mm horizontal spacing. The spread in the three time estimates at each vertical level reflects the uneven top surface of the sample during combustion. Height decrease occurred continuously during the main combustion period, but the 20 mm vertical spacing between the thermocouples gives a stepwise resolution of the height estimations. The height estimation method was verified by manual measurements with a ruler during selected experiments, showing an overall estimated accuracy of the method to be ±10-20 mm.

2.4 Statistical method

In each scenario there were relatively few repetitions of experiments. Shapiro-Wilk W test for normality [21] showed that the results in each group were rarely normally distributed. To quantify possible differences between groups for non-normally distributed groups, a two-tailed Mann-Whitney U test was used [22]. The tested null-hypothesis is that the continuous cumulative distribution functions of the two groups are equal, the alternative hypothesis is that a randomly selected value of one group is likely to be smaller than a randomly selected value of the other group. A significant difference between groups is determined by a significance level

of $p < 0.05$. The statistical analysis was carried out using the Statistica software, version 13 [23].

2.5 Cooling scenarios

Four scenarios were studied. The Background scenario was a point of reference without fuel bed cooling. In scenarios A, B and C, heat was extracted from the fuel bed, with an increasing cooling level from A to B to C.

- Background: No cooling unit in fuel bed
- Scenario A (minimum cooling): Cooling unit in fuel bed, no water in unit
- Scenario B (medium cooling): Cooling unit in fuel bed, water flow started halfway through the external heating period (at t = 6.5 h)
- Scenario C (maximum cooling): Cooling unit in fuel bed, water flow started at the beginning of the experiment (at t = 0 h)

3 Results

In this section, the reader will be introduced to a typical experimental data set. Temperature and mass loss rates for non-extinguished and extinguished experiments will be presented in section 3.1. Total mass loss and discoloration of the fuel will be presented in section 3.2, followed by water temperature and water flow data in section 3.3.

3.1 Temperature and mass loss rate

The first 18 hours of an experiment are shown in Fig. 5. The heater was switched on from 0 h to 13 h, gray shading indicates the external heating period. The sample was slowly heated from below by the aluminum plate (heater, at height 0 mm). As a consequence, the temperature increase in the lower part of the sample (20, 40 mm) was more rapid than in the upper part (60, 80, 100 mm). The temperature stagnation at 70-100 °C and the high mass loss rate during the early phase of the external heating are due to drying of the material. The total mass loss at 13 h was around 35 wt%, which is higher than the 6.3 wt% moisture content of the sample. This indicates that the sample was not only dried, but also underwent other mass consuming processes, such as pyrolysis and partial combustion. The asymmetrical temperature build-up (the three temperature curves for each height level differ systematically) reveals both heat generation in the fuel, and complex air flow patterns within the fuel bed. The center temperatures were lower than those located at the sides due to the proximity of the cooling unit. After the external heating was switched off at 13 h, the heater temperature decreased towards ambient temperature. The sample temperatures also decreased, but more slowly. After 2-3 h, sample temperatures started increasing. This shows initiation of self-sustained smoldering, with heat production in the fuel bed larger than heat losses to the surroundings. Negative mass loss rates were occasionally recorded, as a consequence of condensation of moisture onto the steel pipe, insulation or other

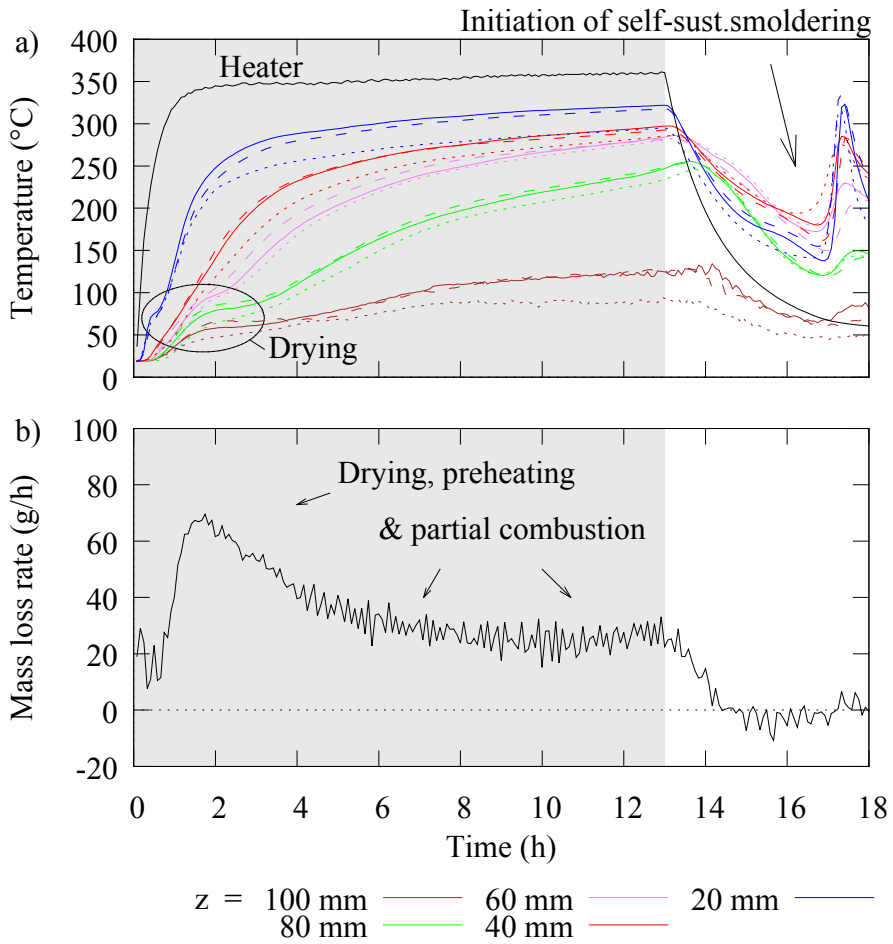

Figure 5 Temperature (top) and mass loss rate (bottom) as a function of time, for the first 18 h of an experiment. Mass loss rate is given as 5 min averages. External heating is indicated by gray shading. Temperature measurement positions are given by the legend below the bottom graph as vertical distance above the heater (20-100 mm). Horizontal positions are given by line type: center is dotted line, left side is full line, right side is dashed line (see Fig. 2). Heater temperature is also given. Center temperatures deviated from side temperatures due to proximity to the cooling unit. Asymmetrical temperature build-up for left vs right side indicate uneven heat generation and complex air flow patterns in the fuel bed. First indication of self-sustained smoldering after the external heating was switched off is indicated by an arrow in the top plot. The full experiment is given under scenario A in Fig. 6.

parts of the experimental set-up and fluctuations in the water flow through the cooling unit.

Background scenario experiments consistently obtained self-sustained smoldering after an external heating duration of 6 hours. For the experiments in scenarios A-C, the same external heating duration did not lead to self-sustained smoldering, due to the introduction of the cooling unit into the fuel bed. This was the case even for scenario A, without water in the cooling unit. To study the feasibility of

Table 1 Experimental parameters and results. *Cooling unit* denotes whether the cooling unit was present in the fuel bed or not. *Heating duration* gives the duration of the external heating. *t(water start)* is given as the time after t = 0 when the water flow through the cooling unit was started. Three result categories are used: Non-extinguished, Extinguished and No smolder. *Obs/Rep* gives the number of observed cases in each category, out of the total number of repetitions in that scenario.

Scenario	Cooling unit	Heating duration	t(water start)	Result category	Obs/Rep
Background	No	6 h	No water	Non-ext	10/10
A (min cooling)	Yes	13 h	No water	Non-ext	6/6
B (medium cooling)	Yes	13 h	6.5 h	Non-ext	6/6
C (max cooling)	Yes	13 h	0 h	Non-ext [1]	7/15
				Extinguished	7/15
				No smolder	1/15

1) Transition from smoldering to flaming (approximately 5 min flame duration) was observed in one of these experiments.

Table 2 Characteristic quantities for each scenario, given as averages with standard deviations for all experiments in that scenario. For scenario C, results are given for each category. T_{max} denotes maximum temperature reached inside the sample during experiments , t_{Tmax} the time to reach that maximum, $\dot{m}_{s,avg}$ and $\dot{m}_{s,peak}$ gives the average and maximum mass loss rate. $\dot{m}_w$ gives the water flow rate through the cooling unit, and ΔT_w gives the water temperature difference. The water data is given for the time period relevant for extinguishment, from the water flow was started until t = 20 h.

Scenario	T_{max} [°C]	t_{Tmax} [h]	$\dot{m}_{s,avg}$ [g/h]	$\dot{m}_{s,peak}$ [g/h]	$\dot{m}_w$ [L/min]	ΔT_w [°C]
Background	574 ± 29	29 ± 2	18 ± 1	227 ± 39	n.a.	n.a.
A: Non-ext	580 ± 36	24 ± 10	20 ± 2	281 ± 42	n.a.	n.a.
B: Non-ext	575 ± 37	23 ± 4	21 ± 1	243 ± 79	0.63 ± 0.04	0.5 ± 0.2
C:						
Non-ext	599 ± 33	34 ± 6	20 ± 1	437 ± 294 [1]	0.65 ± 0.03	0.4 ± 0.2
Extinguished	397 ± 44	18 ± 2	16 ± 1	74 ± 13	0.65 ± 0.03	0.4 ± 0.2
No smolder	n.a.	n.a.	17	69	0.66	0.3

1) Including flaming experiment with mass loss rate peaking at 845 g/h. Excluding the experiment with flaming, $\dot{m}_{s,peak}$ = 302 ± 139 g/h.

using water cooling as an active suppression method, initiation of self-sustained smoldering was necessary. Preliminary experiments showed that a minimum of 13 hours external heating was needed to obtain self-sustained smoldering with the cooling unit in the fuel bed. Still, there was one case in scenario C where even this extended heating period did not lead to self-sustained smoldering. Table 1 gives an overview of the results for the four scenarios studied. Table 2 gives characteristic quantities for each scenario.

The experiments were categorized as follows:

- Non-extinguished (Non-ext): Self-sustained smoldering was initiated and continued till most of the fuel had been consumed (burn-out).
- Extinguished: Self-sustained smoldering was initiated, but extinguished due to the cooling of the fuel bed.
- No smolder: The sample was heated, but no self-sustained smoldering was observed after the external heating was switched off.

Non-extinguished experiments: Typical temperature profiles, mass loss rates and sample heights for non-extinguished experiments for the four studied scenarios are given in Fig. 6. After the heater was switched off, self-sustained smoldering

was observed. Fuel bed temperatures remained around 200-400 °C for 10-30 h, with occasional variations and peaks. In some cases synchronized pulsating temperatures were observed (Scenario A and C in Fig. 6). Details on pulsations are presented in [24,25].

After the period of moderate temperatures within the non-extinguished samples, followed the most intense combustion of the experiments. The time to reach the most intense combustion and maximum temperatures are given in Table 2, for each scenario. Maximum temperatures were registered in the upper parts of the sample (80-100 mm), near the free surface as shown in Fig. 6-top. The sample height (Fig. 6-bottom) decreased during the period of the most intense combustion, as the wood pellets were consumed in the combustion. Trends in mass loss rates (Fig. 6-middle) followed the temperature profiles, peak mass loss rate coincided with temperature peaks. Mass loss rate peaks were around 200-400 g/h (Table 2), or 3-6 g/m^{2}s when averaged over the horizontal cross section-area of the sample. This is similar to mass loss rate peaks found for cotton smoldering in a similar vertical set-up with uninsulated side walls, around 240-270 g/h, or 3-3.3 g/m^{2}s when averaged over their cubic sample cross-section of 150 mm [26].

There were four deviating cases where the most intense combustion occurred directly after the external heating was switched off, instead of after a slow and steady or pulsating period. These cases were 3 of 6 experiments in scenario A and 1 of 6 experiments in scenario B, explaining their larger spread in t_{Tmax} in Table 2. An example may be found in [27]. Another deviating incident was transition to flaming, observed during the most intense combustion of an experiment in scenario C. The flaming lasted for approximately 5 minutes, with mass loss at 845 g/h. While the maximum temperature in the sample was 611 °C, the maximum temperature in the gas above the sample reached 786 °C. This demonstrates flaming combustion, since experiments with no flaming normally had maximum gas temperatures above the sample around 100-150 °C.

The most intense combustion in the non-extinguished experiments was followed by a period of slow and steady combustion in the lower parts of the sample (20 - 60 mm), which at this time were closer to the free surface. In most experiments there were shorter periods towards the end with increased temperature and mass loss rates (see examples in Fig. 6 at 50-52 h for Background, or at 42-45 h for Scenario B). These secondary peaks had higher ratio of temperature to mass loss rate. This is most likely due to a higher char content in the fuel bed, with more intense combustion compared to the first intense combustion peak. The average mass loss rate during the entire experiments was around 20 g/h (Table 2) or 0.31 g/m^{2}s when averaged over the horizontal cross section-area of the sample. Eventually, the entire fuel bed cooled down to ambient temperature. After the experiments the samples consisted of ash and charred pellets. Brittle bridges above voids were observed in the residue piles.

The influence of the cooling unit can be seen by comparing the Background scenario with scenario A, B and C in Fig. 6. During the external heating period, the sample temperatures in the uncooled Background experiments increased faster than in scenario A-C. Also, the mass loss rate was high ($>$ 50 g/h) during most of the external heating period for the Background experiments, while for scenario A-C, the mass loss rate peaked ($>$ 50 g/h) at the beginning of the external heating period, followed by lower mass loss rates ($\sim$10-30 g/h).

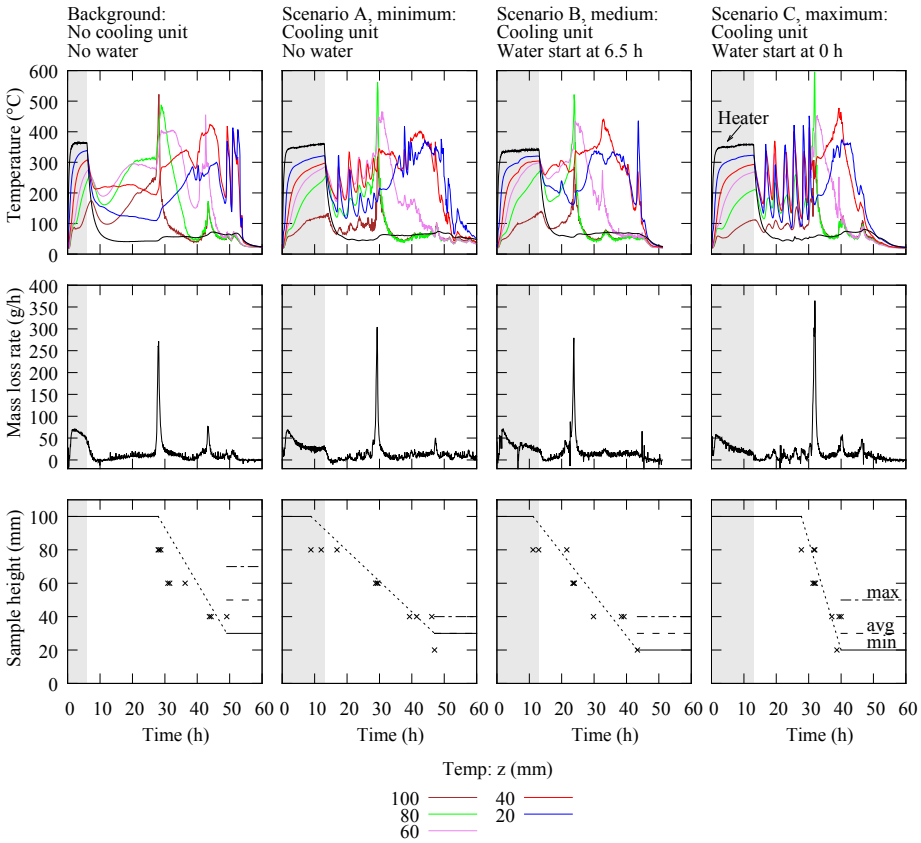

Figure 6 Non-extinguished: Temperature profiles (top), mass loss rate (center) and sample height (bottom) as a function of time, for representative Background and scenario A-C experiments (columns). Mass loss rate is given as 5 min averages. External heating is indicated by gray shading. The heater temperature is indicated. For temperatures, the legend gives vertical height of measurement points as distance above the heater (20-100 mm). For clarity, only one measurement at each vertical height is displayed (the leftmost ones in Fig. 2). Sample heights are approximate, average may overlap with minimum. Details on sample height measurements are given in section 2.3. See the main text for details on temperature and mass loss rate peaks.

Not only the presence of the cooling unit, but also the water flow through the cooling unit clearly affected the net heating of the sample. This can be seen by comparing the temperature build-up at 80 mm height during the external heating period, which was distinctly lower for scenario C compared with scenario A. The mass loss rate during the external heating period was also lowest for scenario C. The influence of the water flow on the temperature profiles and mass loss rates is also evident at 6.5 h in scenario B, the time when the water flow was started, giving abrupt changes in some of the temperatures and a drop in the mass loss rate (due to the added weight of the water in the cooling unit).

Extinguished experiments: Typical temperature profiles and mass loss rates for extinguished experiments are given in Fig. 7. All experiments are from scenario C, as this was the only scenario where extinguishment was obtained. The external

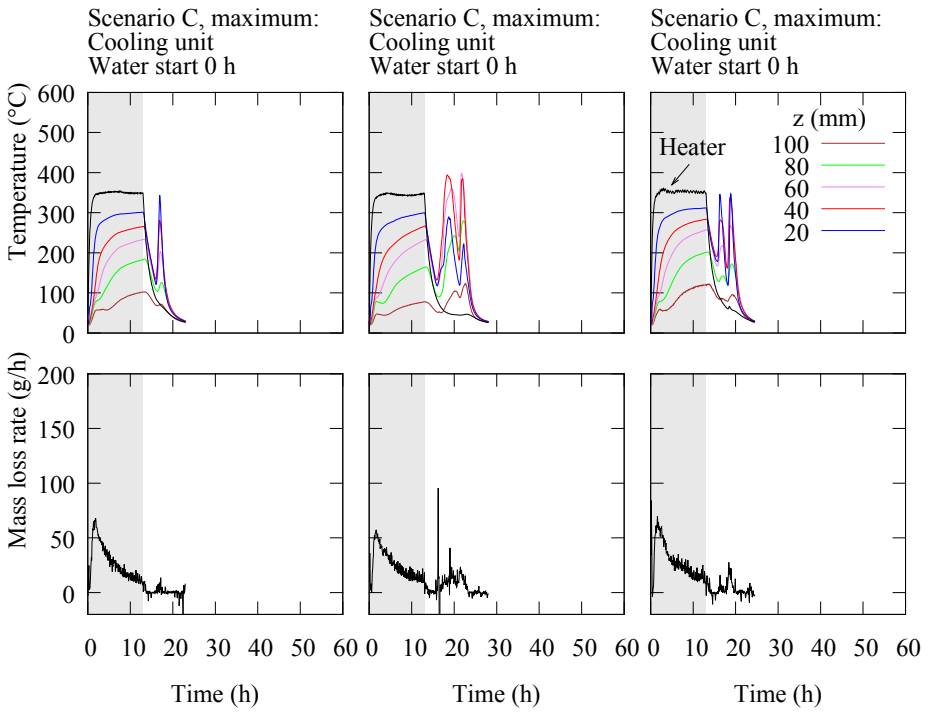

Figure 7 Extinguished: Temperature profiles (top) and mass loss rate (bottom) as a function of time, for representative extinguished experiments, all scenario C. Mass loss rate is given as 5 min averages. External heating is indicated by gray shading. The heater temperature is indicated. For temperatures, the legend gives vertical height of measurement points as distance above the heater (20-100 mm). For clarity, only one measurement at each vertical height is displayed (the leftmost ones in Fig. 2). The y-axis for the mass loss rate is rescaled compared with Fig. 6. The variation in mass loss rate (center graph) around 17 h is discussed in more detail in section 3.3. The sample height did not decrease during the experiment.

heating duration was 13 h, after which the sample cooled down, followed by a temperature increase caused by self-sustained smoldering. This is of importance, as one of the goals of this study was to obtain extinguishment of an ongoing self-sustained smoldering fire. Temperature profiles resembled the first pulsating temperatures of the non-extinguished experiments (Fig. 6) with average peak temperatures of 400 °C (Table 2). In four of the seven extinguished experiments there was one pulsation before extinguishment (Fig. 7-left) with mass loss rate peak during pulsation of 10 g/h. In the three remaining experiments, there were two pulses (Fig. 7-center and right), with mass loss rate peak of 20 g/h. The higher mass loss rate indicates more intense combustion in the second pulse before extinguishment. The highest mass loss rate during the extinguished experiments was measured during the external heating period (around 77 g/h), while the the average mass loss rate during the entire experiments was around 16 g/h (see Table 2), or 0.25 g/m^{2}s when averaged over the horizontal cross section-area of the sample.

After one or two pulses, and without any additional extinguishing efforts other than the continuous water flow through the cooling unit, the fuel bed cooled down to ambient temperature and the smoldering was extinguished. Self-sustained smol-

dering was interrupted before intense smoldering occurred. This is evident by the short period of elevated, but relatively low temperatures compared with the non-extinguished cases in Fig. 6. The low total mass loss also shows that extinguishment was obtained long before burn-out. The sample height did not decrease from the starting height of 100 mm, but often rather increased 10-20 mm by swelling. A large share of the fuel was not burnt (details in section 3.2).

3.2 Total mass loss and discoloration

The total mass loss of the non-extinguished experiments (around 86 wt%) represents a statistically significant higher fuel consumption compared with the extinguished experiments (around 30 wt%), see Fig. 8a. The moisture content in the sample was 6.3 wt%. Thus, even in the extinguished experiments, some fuel was consumed through self-sustained smoldering.

The composition of the residue after the experiments, is given in Fig. 8b. The residue combined with the total mass loss corresponds to the initial mass of the experiment. For the non-extinguished experiments, the residue consisted of black pellets and ash. There were only small differences in the residue composition between the scenarios. For the extinguished experiments, around 27 wt% of the original sample was visually unaffected or negligibly affected by the combustion (9 $\pm$ 2 wt% of the residue was original pellets, 4 $\pm$ 0.3 wt% wood dusts and 14 $\pm$ 1 wt% semi-brown pellets). There were 13 $\pm$ 1 wt% brown pellets and 30 $\pm$ 2 wt% black pellets, in total around 43 wt% visibly affected by the combustion. There was no visually detectable ash, though any ash residue could have mixed with the wood dusts.

Compared with previous experiments using the same set-up but without the cooling unit[18], the residue after the extinguished experiments resembles the residue after experiments with a smaller sample size (60 mm height) where self-sustained smoldering was not observed. Both residues have a high content of black or charred pellets (about 30 wt%). In the previous study, it was probably the high free surface to volume ratio that gave heat losses too high to obtain self-sustained smoldering. In this study, the larger fuel bed is more insulated, enabling self-sustained smoldering, where the cooling unit represents the additional heat loss leading to extinguishment.

3.3 Water temperature and water flow

The water temperature difference (ΔT_w) over the cooling unit is given in Fig. 9, for scenarios with water flow (B and C). The time period (0-30 h) covers the entire duration of the extinguished experiments. The graphs in Fig. 9a represent average values as functions of time. Averages were taken over extinguished experiments in scenario C, over non-extinguished experiments in scenario B, and non-extinguished experiments in scenario C, respectively.

Averaged water temperature difference is given for the time period relevant for studying the cause of extinguishment in Fig. 9b. Tabulated averages are given in Table 2. The time period presented is the first 20 and 25 h of experiments, which is the time period with elevated sample temperatures in the extinguished

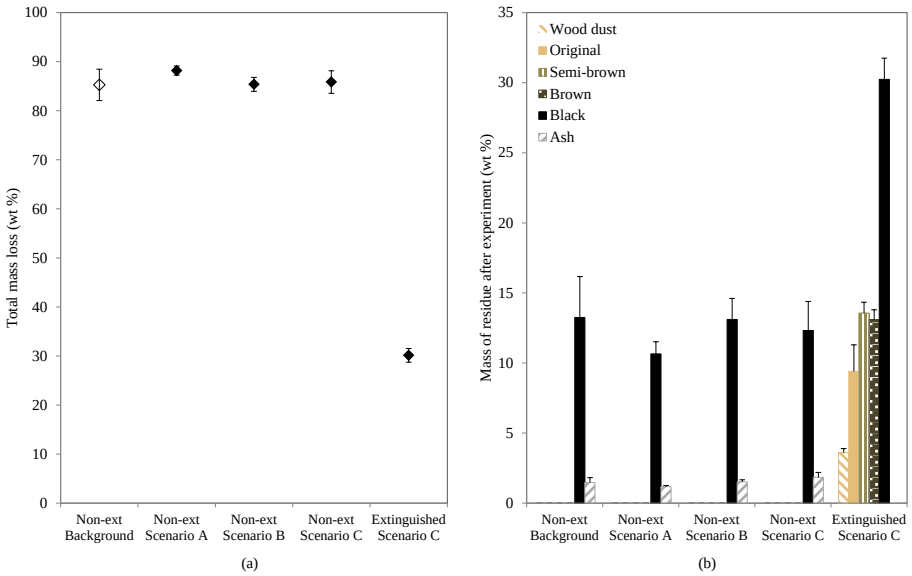

Figure 8 The total mass loss during the experiments (a) and composition of the residue (b) for both non-extinguished and extinguished experiments. Averages for all experiments within each scenario. The sum of the total mass loss during the experiment (a) and the residue after the experiment (b) corresponds to the mass at the start of the experiment. Background scenario is included with unfilled marker in (a) to emphasize the shorter external heating duration (6 h vs 13 h), possibly affecting the total mass loss.

experiments (see Fig. 7). Average water temperature difference was higher for scenario B, but not significantly.

For scenario C in Fig. 9a, notice the similarities between non-extinguished and extinguished experiments during the first 16-18 h. After this, the gradually more intense combustion in the non-extinguished experiments (see Fig. 6) was also reflected in the water temperatures, while the experiments resulting in extinguishment gradually cooled down (see Fig. 7). In scenario B, the ΔT_w was higher from the time the water flow was started at 6.5 h and remained higher. This reflects the elevated temperatures in the fuel at the time of water flow start.

The flow rate through the cooling unit varied slightly during an experiment, but there was no difference between the average flow rate of the non-extinguished and the extinguished experiments in scenario C, as given in Table 2. The average flow in scenario B was slightly lower. Sudden flow rate variations from the municipal water supply could give a recoil impact on the mass loss data due to the added weight of the water, as seen in the mass loss rate around 17 h in Fig. 7-center.

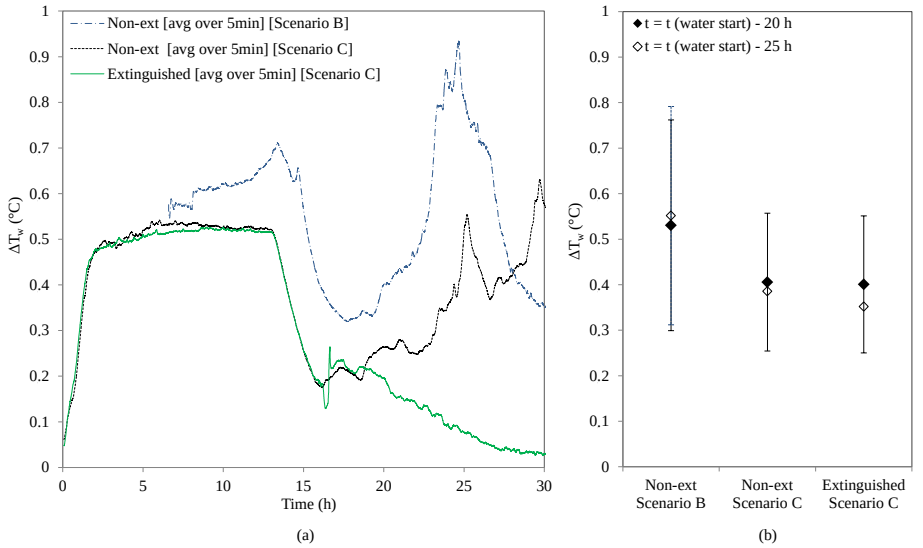

Figure 9 Water temperature difference between inlet to and outlet from the cooling unit (ΔT_w), data given as (a) ΔT_w for 5 min moving averages as a function of time and as (b) overall ΔT_w averages and standard deviations. The time period included is from the time when water flow was started (see $t(waterstart)$ in Table 1) to t = 20 h (filled markers) and t = 25 h (unfilled markers). Each graph (a) and point (b) represent averages over all experiments in the category.

4 Discussion

The successful extinguishment of self-sustained smoldering in biomass demonstrated in this study is innovative. The heat extraction from the fuel bed was in some cases sufficient to quench self-sustained smoldering. Furthermore, the cooling affected the combustion when complete extinguishment was not obtained. The results should be of interest for large-scale applications. In this section, the effect of the water cooling on the combustion will be discussed. Also, the scalability and application of the results will be explored.

4.1 Increased cooling: increased predictability

Even when the cooling was insufficient to obtain extinguishment, variations in the combustion pattern between scenarios were observed. The most intense smoldering period during an experiment is given by peaks in sample temperatures and mass loss rate, see Fig. 6. The temperature maximum during this period was not statistically significant different between the scenarios, see Table 2. The time to reach that temperature maximum (t_{Tmax}), on the other hand, provides information on the activity in the fuel bed. For scenario A, there was a large spread in the t_{Tmax} data, as some experiments had the most intense combustion period directly after the external heating was switched off, others much later. This large variation for the same starting parameters reflects the inherent stochastic behavior of smoldering fires.

Introducing water flow in the cooling pipe (scenarios B and C) gave a more steady and predictable combustion, with a smaller variations in t_{Tmax} compared to scenario A. There were also indications (although not statistically significant) that increased cooling gave increased t_{Tmax}. The increase in t_{Tmax} was observed as the water flow duration was increased from scenario B (water flow from 6.5 h) to scenario C (water flow from the start of the experiment). Notice that there was no statistically significant difference when comparing scenario A vs B, or scenario A vs C, due to the large spread in the data for scenario A.

These results indicate that increased cooling could both give higher predictability and increased time to reach the most intense combustion period. This can be of importance from a risk perspective, as it would allow more time for alternative suppression methods to be implemented. However, the consequence of delaying the intense combustion period could be a fuel bed with more char, prone to transition to flaming, as demonstrated by one experiment in scenario C.

4.2 Cooling was not limited by water flow

The cause of extinguishment will now be explored. The water temperature difference through the cooling unit, given in Table 2 and detailed in Fig. 9, indicate that cooling was not limited by the water flow rate or the temperature of the water. The water temperatures closely followed the temperatures within the sample, thus the heat transfer from the fuel bed to the cooling unit was larger when the sample was warm, with more heat extracted from the sample, as expected. The water temperature difference (typically around 0.4-0.5 °C) was low in comparison to the combustion temperatures within the sample. This shows that the water had capacity to remove more heat.

Since cooling was not limited by the water flow, the limitation must mainly lie in the transportation of the heat from combustion sites to the centrally located cooling unit. In these experiments, it was essential for extinguishment that a temperature gradient was established in the sample at an early stage. This was demonstrated in Fig. 9, in that when the water flow was started simultaneously with the external heating (in scenario C), the water cooling subdued the combustion, and extinguishment was obtained in 7 of 15 cases. This was the only scenario that resulted in extinguishment. When the water flow was started at a later stage (at 6.5 h in scenario B), there was higher heat extraction per time (higher $\Delta \mathrm{T_w}$), but the water cooling was not sufficient to build up the necessary temperature gradient. Consequently, the combustion was not quenched.

4.3 Analysis of cooling

The cooling must be key to understand the cause of extinguishment, in particular why 7 experiments did not extinguish and 7 experiments resulted in extinguishment within the same scenario C.

In this section, the heat production ($\dot{\mathrm{q}}_{\mathrm{prod}}$) from the smoldering combustion,

$$\dot{q}_{\mathrm{prod}} = \dot{m}_{\mathrm{s}}\, H_{\mathrm{c}} \tag{1}$$

is therefore compared with the cooling, that is, the heat loss ($\dot{q}_{cool}$) to the cooling unit,

$$\dot{q}_{cool} = \dot{m}_w \, \Delta T_w \, C_{p,w} \, . \quad (2)$$

Here, $\dot{m}_s$ is the mass loss rate of the sample, H_c is the effective heat of combustion of the sample (set to 6 MJ/kg, see discussion below), $\dot{m}_w$ is the water flow rate, ΔT_w is the temperature difference between water entering and leaving the cooling unit, $C_{p,w}$ is the specific heat capacity of water (4.18 J/gK [28]). The heat production (Eq. 1) and heat loss to the cooling unit (Eq. 2) are here given for representative extinguished (Fig. 10a) and non-extinguished (Fig. 10b) experiments in scenario C, based on measured experimental data. These calculations are approximations for heat production and heat loss. The time period given corresponds to the entire duration of the extinguished experiments, and the same time span is presented for the non-extinguished, although these experiments lasted longer. Negative heat production is due to occasional negative mass loss rates, as the recorded mass data includes the entire set-up including condensation of moisture, as described in section 3.1.

During the external heating period (0-13 h) the imposed heating on the sample gave high mass loss, and thereby an excess in the calculated heating (Eq. 1) compared with cooling (Eq. 2), for both extinguished and non-extinguished cases. This is explained by evaporation of water, which leads to mass loss that is not connected to heat production. After the external heating was switched off (at 13 h), all heat generation occurred in the sample. During this period, the cooling was estimated to be in the range 5-20 W while the heat production was in the range 0-60 W, see Fig. 10. The cooling and heat production of the extinguished vs the non-extinguished cases were similar at the beginning of the experiments. Starting from 20 h into the experiments, a difference appeared. The heat production became increasingly prominent for the non-extinguished experiments, shown by asterisks (*) marking large heat excess in Fig. 10. The difference was most distinct when comparing the non-extinguished (Fig. 10 e-h) with the extinguished experiments with only one temperature pulse before extinguishment (Fig. 10c-d). The experiments with two temperature pulses before extinguishment (Fig. 10a-b) were more similar to the non-extinguished cases. Eventually, the extinguished cases cooled down to ambient temperature. The non-extinguished cases, on the other hand, continued to alternate between periods with high and low heat excess, reflecting the pulsating temperatures and mass loss rates in the fuel bed (shown in Fig. 6, further details on the pulsating phenomenon is presented in [24]). There was a gradually more intense combustion, eventually leading to temperature and mass loss peaks.

There is a large uncertainty in the value for the effective heat of combustion (H_c) used for calculation of the heat production (Eq. 1). Firstly, for any given fuel the effective heat of combustion for smoldering processes is poorly known. Secondly, the exact composition of the fuel is not known, as this changes as the experiments proceed. The total heat of combustion with unlimited oxygen access, may be measured (upper and lower calorific values, see section 2.1). However, the *effective* heat of combustion for smoldering, with incomplete combustion and possibly also limited oxygen supply, is very uncertain. Only a limited number of values regarding the effective heat of combustion for smoldering has been published. The

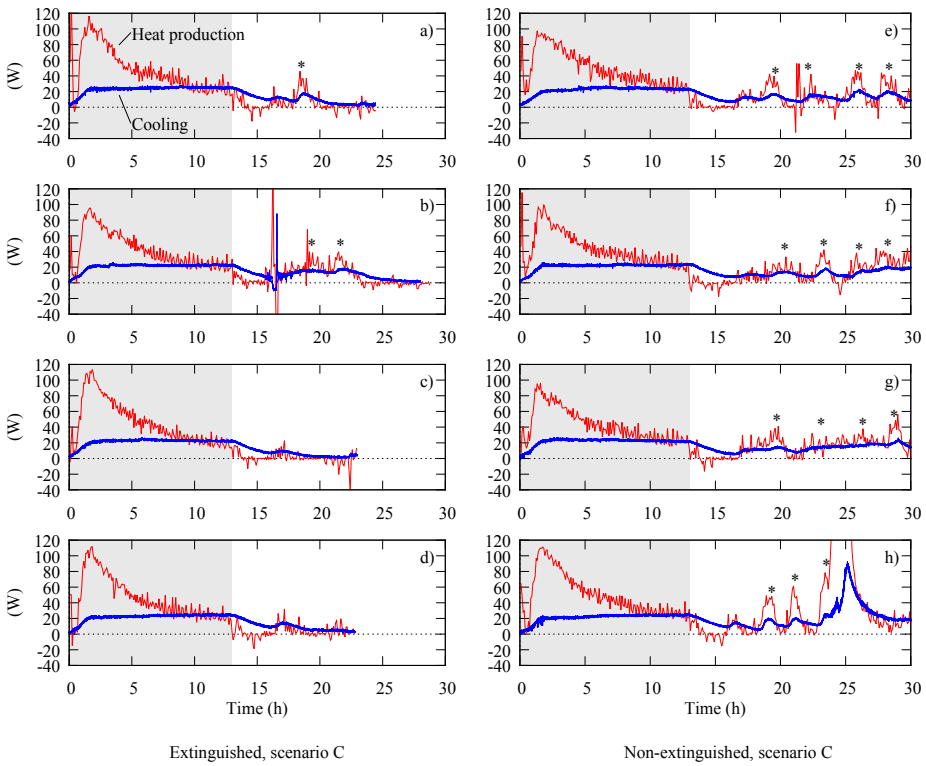

Figure 10 Calculated heat production from the smoldering combustion (Eq. 1, red lines) and heat loss to the cooling unit (Eq. 2, blue lines), for 4 representative extinguished cases (a-d) and 4 representative non-extinguished cases (e-h), all for scenario C with maximum cooling. External heating is indicated by gray shading, during this period, evaporation of water leads to mass loss not connected to heat production. Large heat excess after the external heating period (from 13 h) is marked with asterisks (*). Corresponding temperature and mass loss rate profiles for (a-c) are given in Fig. 7 and for (e) in Fig. 6 under Scenario C.

reported values vary significantly and this variability has not been accounted for[2]. The reported effective heat of combustion for smoldering varies from extremely low values of 1.05 MJ/kg for PUR foams [29], 1.7 MJ/kg for newspaper [30], and 2.1 MJ/kg for cotton [29], to 6.7 MJ/kg for cotton lamp wick [30] and a range of 6-12 MJ/kg for solid woods [3,31]. Differences in experimental geometries and air flows affect the measured values: increased forced air flow gives higher effective heat of combustion. In this study, there is no forced air flow, and the lowest reported value of 6 MJ/kg [3,31] for solid wood is therefore chosen as most representative. The second concern is that the fuel changes properties as it dries, decompose and is combusted. Despite the changes in the fuel, the effective heat of combustion is kept constant, as the exact composition in the fuel bed at various stages during an experiment is not known.

[2] According to personal e-mail correspondence with Dr. Vytenis Babrauskas, and his not yet published report "Engineering guidance for smoldering fires".

The consequence of an estimated effective heat of combustion is that the heat production presented in Fig. 10 is over- or underestimated compared to the true values. If the chosen effective heat of combustion is too large, then the heat excess (marked by asterisks (*) in Fig. 10) is overestimated, and the cooling unit is actually able to extract a larger amount of the produced heat. If, on the other hand, the chosen value for effective heat of combustion is too small, then the smoldering fuel actually produces more heat than what is apparent in Fig. 10, the heat production should be stretched, meaning that it would be easier to distinguish the non-extinguished cases from the extinguished. The effective heat of combustion for smoldering fires in biomass would benefit from further studies, which should include parameters such as fuel composition and moisture content. It would be beneficial if the fuel could be produced to order, enabling a systematic variation of wood composition and moisture content.

Regardless of the exact choice of effective heat of combustion for the fuel, these calculations show that within the same scenario, there are only minor differences between heat production and cooling. Still, within the same scenario C, half the cases resulted in extinguishment and the other half did not. It could therefore be speculated that the combustion process in scenario C is at a balance point between an active combustion and an extinguished system, with small random variations in the combustion or in the water flow determining the outcome. These marginal differences emphasize the susceptibility of smoldering fires to variations in external and local conditions.

4.4 Scalability and application

If cooling is to be used to extinguish or control smoldering fires in full-scale industrial settings such as silos, feasible upscaling options from laboratory scale to industrial must be evaluated. One upscaling option using a cooling unit in a silo is presented in this section.

A silo with similar dimensions as the silo involved in a serious fire in Esbjerg, Denmark in 1998-99 [2] will be used as an example. Silo height of 85 meter, silo cell diameter of 3 meter will be used in calculations, see Fig. 11. An example cooling unit consisting of a 0.2 m diameter cylinder is considered. The cooling ($\dot{q}_{cool}$) needed for the cylindrical cooling unit is given by Fourier's law,

$$\dot{q}_{cool} = 2\,\pi\,\kappa\,h\,\frac{T_{fuel} - T_{water}}{ln(r_1/r_2)} \tag{3}$$

where κ is the thermal conductivity of the wood pellets, h is the height of the silo, T_{fuel} is the fuel bed temperature, T_{water} is the water temperature, r_1 is the cooling unit radius and r_2 is half the silo radius, see Fig. 11. The lowest measured thermal conductivity for the ground wood pellets is chosen (0.15 W/mK), as this is closest to the values found for similar, whole wood pellets by Guo et al (0.146-0.192 W/mK) [32].

A case with constant temperatures in the fuel bed is studied, with maximum temperature midway between the cooling unit and outer wall (dotted line in Fig. 11). A stationary situation with linear temperature decrease is assumed, as is heat transfer dominated by conduction (i.e. radiation and convection is not considered in this estimation).

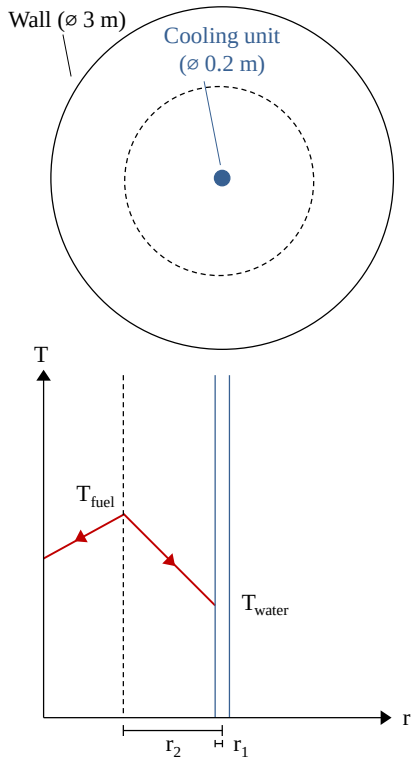

Figure 11 Top view of a silo with a water-cooled pipe in the center (top) and the temperature as a function of radial distance (bottom). The dotted line represents the position of the maximum fuel bed temperature in this example.

With typical bulk self-heating temperature for wood pellets $T_{\text{fuel}} = 50$ °C [16, 32], water temperature $T_{\text{water}} = 16$ °C as in this study, the heat transported to the cooling pipe is around 1300 W, using Eq. 3. To obtain this cooling level, the necessary water flow rate would be around 0.8 kg/s, or 50 L/min, from Eq. 2, using a water temperature difference as measured in this study (around 0.4 °C). On the other hand, with a typical fuel bed temperature during self-sustained smoldering of 400 °C, as observed in this study, the necessary water flow rate is around 9 kg/s, or 550 L/min.

Especially for prevention of escalation of low fuel bed temperatures, the estimated water flow rate values are well within what can be an expected water supply capacity at an industrial site. Still, the total water consumption would be high compared to for instance water consumption in a domestic household. Hence, water cooling could be feasible but not necessarily practical as a preventive large-scale measure. A temperature gradient in the fuel bed must be established sufficiently early to prevent escalation, as discussed in section 4.2. Cooling as an active suppression method is therefore less feasible. This also limits possible benefits of using more efficient cooling units with larger surface to volume ratios, for instance by using fins. Other cooling unit geometries could be considered, such as cooling of the container walls, or spirals as cooling units, or multiple U-shaped loops. For

practical applications, a cooling unit positioned within a storage unit, would have to sustain severe mechanical loads without breaking.

In these small-scale experiments, the imposed external heating to this sample was strong and fast, compared with self-heating temperatures in bulk biomass. If ignition were caused by an external ignition source, for instance by a glowing ember carried into the silo via a fuel supply band, the temperature could have been in a similar range as the heater, or higher, but the size of the hot object much smaller. Thus, this study is a small-scale proof of concept of the method, and further studies are needed to evaluate the feasibility of using similar systems as active or passive extinguishing methods.

Lastly, the residue from the extinguished experiments consisted of a large share of charred pellets, see section 3.2. If required, these charred pellets could be reused as fuel with a higher calorific value than the original pellets. The charred pellets resemble torrefied biomass, which is charred through thermal treatment [33]. The heat extraction system demonstrated here could potentially inspire applications outside fire prevention, for instance as a supplement to torrefaction.

5 Conclusion

An experimental study using a laboratory-scale set-up has been performed, to investigate the feasibility of using water cooling as an extinguishing system for smoldering fires. Wood pellets were used as fuel, sample size was 1.25 kg, 1.8 liters. The set-up consisted of a side-insulated steel cylinder heated from below with natural convection at the top. A cooling unit was used, consisting of a 4.76 mm diameter U-shaped copper pipe centrally located in the sample. Cooling was obtained without direct contact between water and fuel, thus avoiding challenges with swelling of the pellets, water channeling and water run-off. The study demonstrates that water cooling, without direct contact between water and fuel, can be used as an extinguishing system at laboratory-scale.

The study shows that the cooling unit, even without water flow, significantly affected the heating processes in the sample. To obtain self-sustained smoldering in the fuel bed, the duration of the external heating had to be significantly increased. This demonstrates that even moderate cooling could affect initiation of smoldering.

Extinguishment was obtained in half the cases in which the water flow was started at the same time as the external heating. For the experiments with no water flow, or where the water flow was started at a later stage, extinguishment was not obtained. This indicates that, water cooling should be activated before any temperature escalation in the fuel bed, and that water cooling is not well-suited for late-stage suppression.

Extinguishment was obtained at an early stage in the smoldering process, as demonstrated both by the temperature profiles in the sample and by the significant reduction in the fuel consumed during the process. For the non-extinguished cases, increased cooling led to a more steady and predictable combustion, the most intense combustion period could be delayed. If applicable to large-scale, a delay in escalation of temperatures by heat removal would provide firefighters with more time to implement alternative extinguishing measures.

The heat loss to the cooling unit during the period before extinguishment was in the range 5-20 W, while the heat production in the sample was in the range

0-60 W. At this balance point between intense combustion and extinguishment, apparently only marginal differences distinguished between extinguished and non-extinguished cases. Slight variations in the combustion could cause the reaction to tip one way or the other.

Upscaling the heat extraction to an industrial-scale silo could be feasible, and this should be investigated further. Furthermore, it would be useful to explore other cooling unit geometries. Alternative application areas could be considered, such as well-controlled production of charred pellets.

This is the first experimental study to demonstrate that extinguishment of smoldering fires in biomass can be obtained by the use of heat extraction (cooling) from the fuel.

Acknowledgements

References

1. Koppejan, J., Lönnermark, A., Persson, H., Larsson, I., Blomquist, P.: Health and Safety Aspects of Solid Biomass Storage, Transportation and Feeding. Tech. Rep. Task 40, IEA Bioenergy (2013). URL http://urn.kb.se/resolve?urn=urn:nbn:se:ri:diva-5595
2. Krause, U.: Fires in silos: hazards, prevention, and fire fighting. John Wiley & Sons, Germany (2009). URL https://doi.org/10.1002/9783527623822
3. Rein, G.: Smoldering Combustion. In: M.J. Hurley et al (ed.) SFPE Handbook of Fire Protection Engineering, vol. 1, 5th edn., pp. 581–603, Chapter 19. Springer, New York (2016). URL https://doi.org/10.1007/978-1-4939-2565-0_19
4. Rein, G.: Smouldering combustion phenomena in science and technology. International Review of Chemical Engineering **1**, 3–18 (2009). URL http://www.era.lib.ed.ac.uk/handle/1842/1152
5. Ogle, R.A., Dillon, S.E., Fecke, M.: Explosion from a smoldering silo fire. Process Safety Progress **33**(1), 94–103 (2014). DOI 10.1002/prs.11628. URL http://dx.doi.org/10.1002/prs.11628
6. Koerth-Baker, M.: How Do You Put Out A Subterranean Fire Beneath A Mountain Of Trash? (2016). URL http://fivethirtyeight.com/features/how-do-you-put-out-a-subterranean-fire-in-a-mountain-of-trash
7. Sperling, T., Abedini, A.R.: Report on subsurface self sustaining exothermic reaction incident at Bridgeton Landfill, with a focus on causes, suppression actions taken and future liabilities. Tech. Rep. LFCI – PRJ14-010, Landfill Fire Control Inc. (LFCI), British Colombia, Canada (2015). URL http://dnr.mo.gov/env/swmp/facilities/docs/lfci_report_bridgetonlf.pdf
8. Tuomisaari, M., Baroudi, D., Latva, R.: Extinguishing smouldering fires in silos, Brandforsk project 745-961. Tech. Rep. VTT publication 339, Technical Research Centre of Finland, Finland (1998). URL http://www.vtt.fi/inf/pdf/publications/1998/P339.pdf
9. Hadden, R., Rein, G.: Burning and Water Suppression of Smoldering Coal Fires in Small-Scale Laboratory Experiments. In: Coal and Peat Fires: A Global Perspective, vol. 1, pp. 317–326, Chap 18. Elsevier, Amsterdam, Netherlands (2011). URL https://doi.org/10.1016/B978-0-444-52858-2.00017-7
10. Ramadhan, M.L., Palamba, P., Imran, F.A., Kosasih, E.A., Nugroho, Y.S.: Experimental study of the effect of water spray on the spread of smoldering in Indonesian peat fires. Fire Safety Journal **91**, 671–679 (2017). DOI 10.1016/j.firesaf.2017.04.012. URL http://dx.doi.org/10.1016/j.firesaf.2017.04.012
11. Göransson, U., Husted, B.: Can water mist be used to extinguish deep-seated cellulose fibre smouldering fires? Experiments and calculations. pp. 359–364. Interscience Communications, Interflam, Royal Holloway College, University of London (2007). URL http://lup.lub.lu.se/record/764594
12. Seow, J.: Fire fighting foams with perfluorochemicals - environmental review. Tech. rep., Hemming Information Services, Department of Environment and Conservation Western Australia, Australia (2013). URL http://www.hemmingfire.com/news/get_file.php3/id/287/file/Seow_WA-DEC_PFCs_Firefighting_Foam_final_version_7June2013.pdf

13. Moody, C.A., Field, J.A.: Perfluorinated surfactants and the environmental implications of their use in fire-fighting foams. Environmental science & technology **34**(18), 3864–3870 (2000). DOI 10.1021/es991359u. URL https://doi.org/10.1021/es991359u
14. Larsson, I., Lönnermark, A., Blomqvist, P., Persson, H.: Measurement of self-heating potential of biomass pellets with isothermal calorimetry. Fire and Materials **41**(8), 1007–1015 (2017). DOI 10.1002/fam.2441. URL http://dx.doi.org/10.1002/fam.2441
15. Schmidt, M., Wanke, C., Krause, U.: Determination of Measurement Uncertainties in Adiabatic Hot-Storage Experiments for Reactive Dusts. Chem. Eng. Technol. **36**(10), 1764–1772 (2013). DOI 10.1002/ceat.201300068. URL http://dx.doi.org/10.1002/ceat.201300068
16. Larsson, I., Lönnermark, A., Blomqvist, P., Persson, H., Bohlén, H.: Development of a screening test based on isothermal calorimetry for determination of self-heating potential of biomass pellets. Fire and Materials **41**(8), 940–952 (2017). DOI 10.1002/fam.2427. URL https://doi.org/10.1002/fam.2427
17. Steen Hansen, A., Mikalsen, R.F., Jensen, U.E.: Smouldering combustion in loose-fill wood fibre thermal insulation. An experimental study. Fire Technology pp. 1–24 (2018). DOI 10.1007/s10694-018-0757-4. URL https://doi.org/10.1007/s10694-018-0757-4
18. Madsen, D., Wanke, C., Mikalsen, R.F., Haraldseid, I., Villacorta, E., Hagen, B.C., Krause, U., Kleppe, G., Frette, V., Husted, B.: Emerging Risks in Smoldering Fires: Initial Results from the EMRIS Project. pp. 1345–1356. Interscience Communications, Interflam, Windsor, UK (2016). URL https://www.researchgate.net/publication/306078503
19. Villacorta, E., Haraldseid, I., Mikalsen, R.F., Hagen, B.C., Erland, S., Kleppe, G., Krause, U., Frette, V.: Onset of self-sustained smoldering fire in wood pellets: An experimental study (manuscript)
20. Wickström, U.: Chapter 9. In: Temperature Calculation in Fire Safety Engineering. Springer, Switzerland (2016). URL https://doi.org/10.1007/978-3-319-30172-3. 10.1007/978-3-319-30172-3
21. Shapiro, S.S., Wilk, M.B.: An analysis of variance test for normality (complete samples). Biometrika **52**(3/4), 591–611 (1965). DOI 10.2307/2333709. URL https://doi.org/10.2307/2333709
22. Mann, H.B., Whitney, D.R.: On a test of whether one of two random variables is stochastically larger than the other. Ann. Math. Stat. **18**(1), 50–60 (1947). DOI 10.1214/aoms/1177730491. URL https://doi.org/10.1214/aoms/1177730491
23. Dell Inc: Dell Statistica (data analysis software system) (2016). URL software.dell.com
24. Mikalsen, R.F.: Fighting flameless fires - Initiating and extinguishing self-sustained smoldering fires in wood pellets. Doctoral thesis, Otto von Guericke University Magdeburg, Magdeburg, Germany (2018). DOI 10.13140/RG.2.2.34666.16329. URL http://www.diva-portal.org/smash/get/diva2:1251941/FULLTEXT01.pdf
25. Mikalsen, R.F., Hagen, B.C., Frette, V.: Synchronized smoldering combustion. EPL **121**(5), 50002,p1–p6 (2018). DOI 10.1209/0295-5075/121/50002. URL https://doi.org/10.1209/0295-5075/121/50002
26. Hagen, B.C.: Onset of smoldering and transition to flaming fire. PhD thesis, Bergen University, Bergen (2013). URL http://hdl.handle.net/1956/6993
27. Mikalsen, R.F., Hagen, B.C., Steen-Hansen, A., Frette, V.: Extinguishing smoldering fires in wood pellets through cooling. 5th Magdeburg Fire and Explosions Days 2017, Otto-von-Guericke-University, Magdeburg, Germany (2017). DOI 10.978.300/0562013. URL http://dx.doi.org/10.978.300/0562013
28. Incropera, F.P., Dewit, D.P., Bergman, T.L., Lavine, A.S.: Appendix A. In: Foundations of heat transfer, 6th edn., pp. 899–924. John Wiley & Sons, Singapore (2013)
29. Quintiere, J.G., Birky, M., Macdonald, F., Smith, G.: An analysis of smoldering fires in closed compartments and their hazard due to carbon monoxide. Fire and Materials **6**(3–4), 99–110 (1982). DOI 10.1002/fam.810060302. URL https://doi.org/10.1002/fam.810060302
30. Hotta, H., Oka, Y., Sugawa, O.: Interaction between hot layer and updraft from a smoldering fire source, Part I An experimental approach. Fire Sci. Techn. **7**(2), 17–25 (1987). DOI 10.3210/fst.7.2_17. URL https://doi.org/10.3210/fst.7.2_17
31. Ohlemiller, T., Shaub, W.: Products of Wood Smolder and Their Relation-to Wood-Burning Stoves. Tech. Rep. NBSIR 88-3767, US Department of Commerce, National Bureau of Standards, Gaithersburg, MD, USA (1988). URL http://fire.nist.gov/bfrlpubs/fire88/PDF/f88017.pdf

32. Guo, W., Lim, C.J., Bi, X., Sokhansanj, S., Melin, S.: Determination of effective thermal conductivity and specific heat capacity of wood pellets. Fuel **103**(Supplement C), 347–355 (2013). DOI 10.1016/j.fuel.2012.08.037. URL http://www.sciencedirect.com/science/article/pii/S0016236112006746
33. Stelte, W., Sanadi, A.R., Shang, L., Holm, J.K., Ahrenfeldt, J., Henriksen, U.B.: Recent developments in biomass pelletization–A review. BioResources **7**(3), 4451–4490 (2012). DOI 10.15376/biores.7.3.4451-4490. URL https://doi.org/10.15376/biores.7.3.4451-4490

Fig1


10 mm

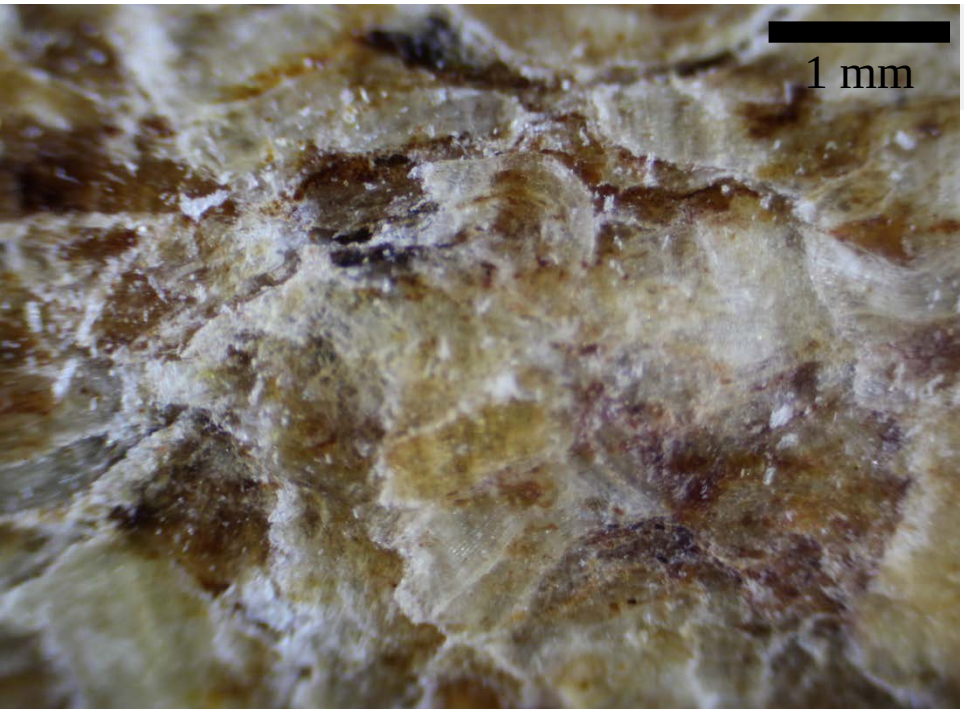
1 mm

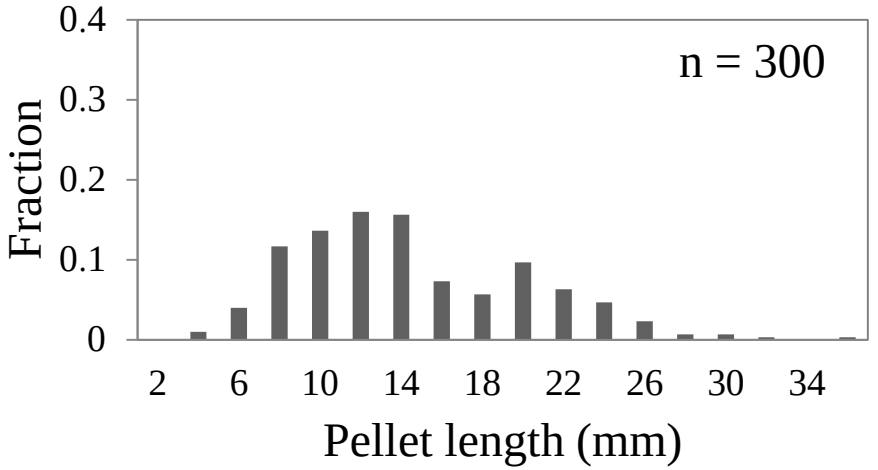
n = 300
Fraction
0.4
0.3
0.2
0.1
0
2
6
10
14
18
22
26
30
34
Pellet length (mm)

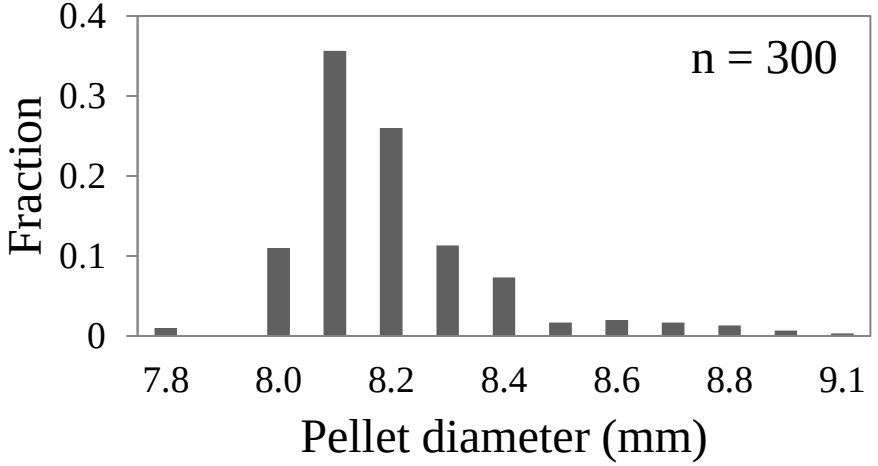
n = 300
Fraction
0.4
0.3
0.2
0.1
0
7.8
8.0
8.2
8.4
8.6
8.8
9.1
Pellet diameter (mm)

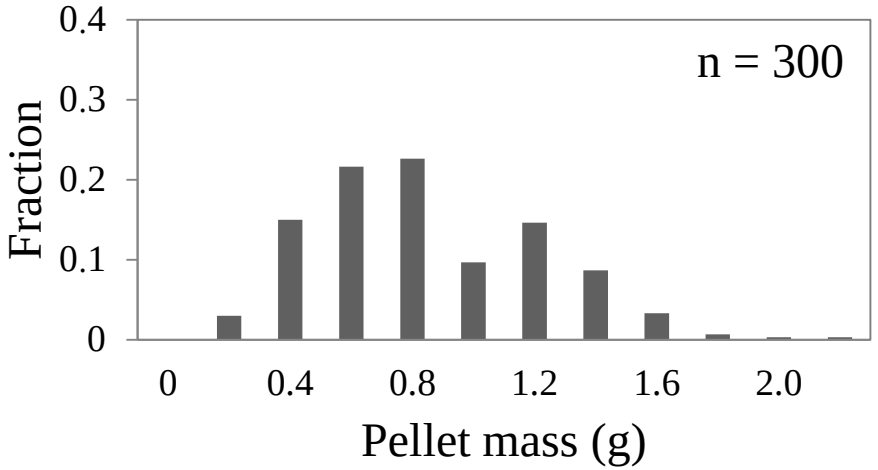
n = 300
Fraction
0.4
0.3
0.2
0.1
0
0
0.4
0.8
1.2
1.6
2.0
Pellet mass (g)


EMRIS

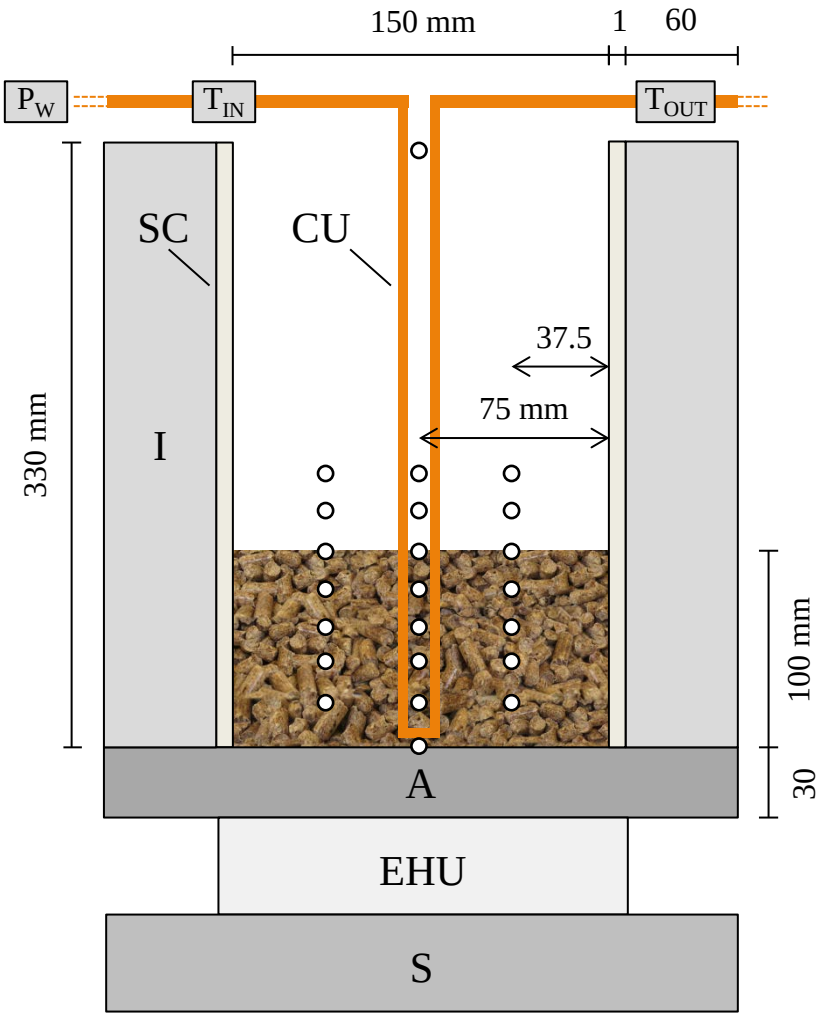
150 mm
1
60
P_W
T_{IN}
T_{OUT}
SC
CU
I
37.5
75 mm
330 mm
100 mm
30
A
EHU
S


a)
Top view of set-up

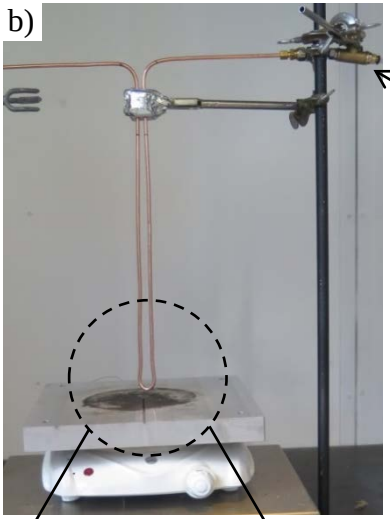
b)


c)
$T_{IN/OUT}$


d)
inch
2m


e)
2m

Fig4

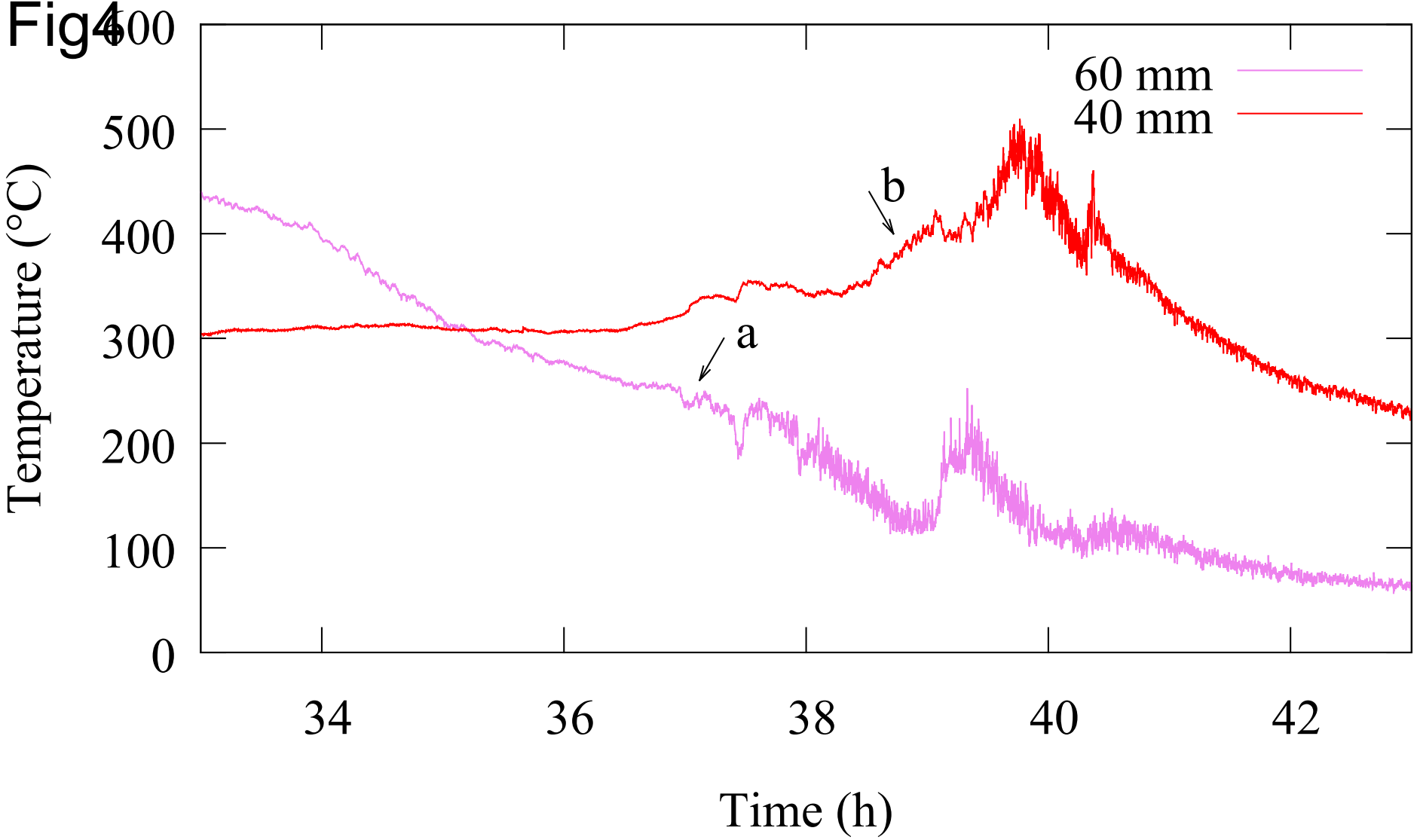
600
500
400
300
200
100
0
Temperature (°C)
34
36
38
40
42
Time (h)
60 mm
40 mm
a
b

Fig5

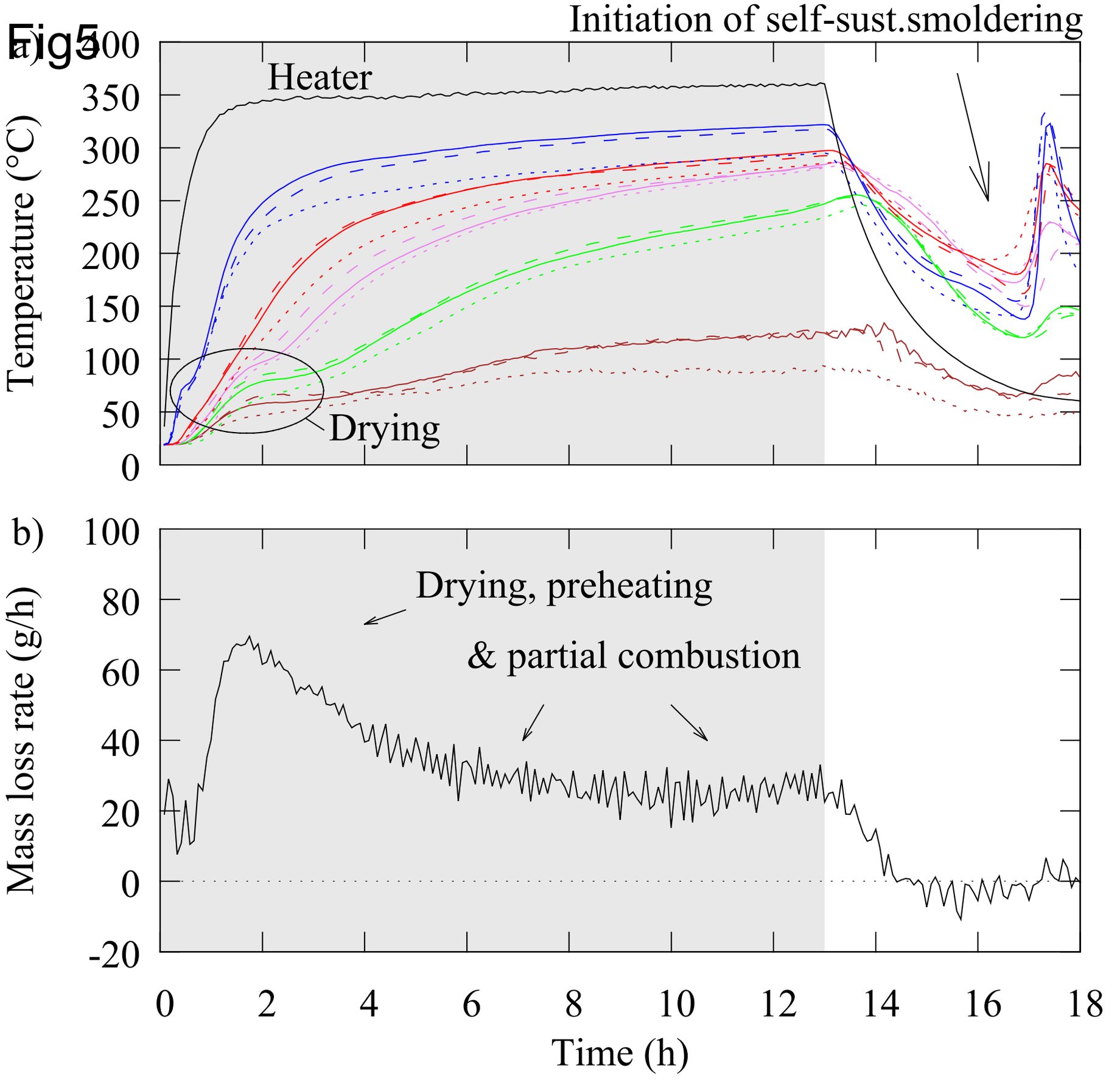
Initiation of self-sust.smoldering
a)
Heater
Drying
Temperature (°C)
0
50
100
150
200
250
300
350
b)
Drying, preheating
& partial combustion
Mass loss rate (g/h)
-20
0
20
40
60
80
100
0
2
4
6
8
10
12
14
16
18
Time (h)
z = 100 mm
80 mm
60 mm
40 mm
20 mm

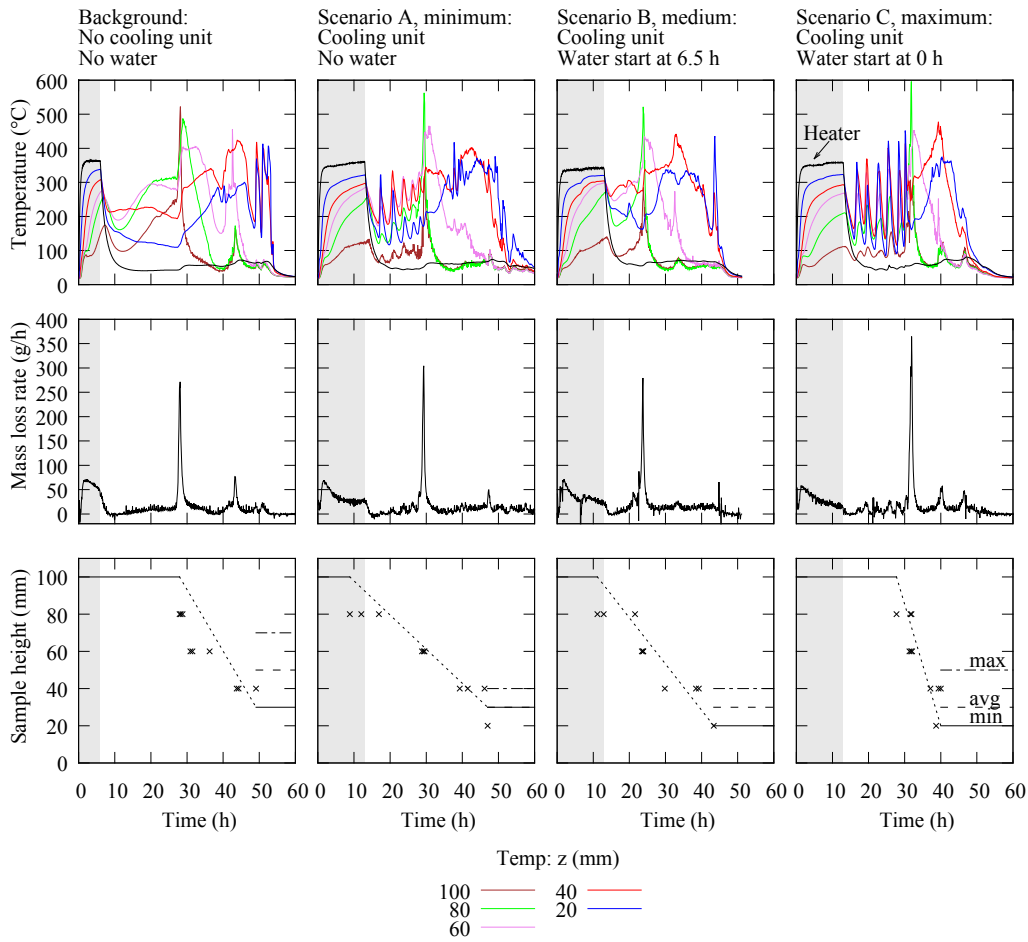
Background:
No cooling unit
No water
Scenario A, minimum:
Cooling unit
No water
Scenario B, medium:
Cooling unit
Water start at 6.5 h
Scenario C, maximum:
Cooling unit
Water start at 0 h
Heater
Temperature (°C)
Mass loss rate (g/h)
Sample height (mm)
max
avg
min
Time (h)
Temp: z (mm)
100
80
60
40
20

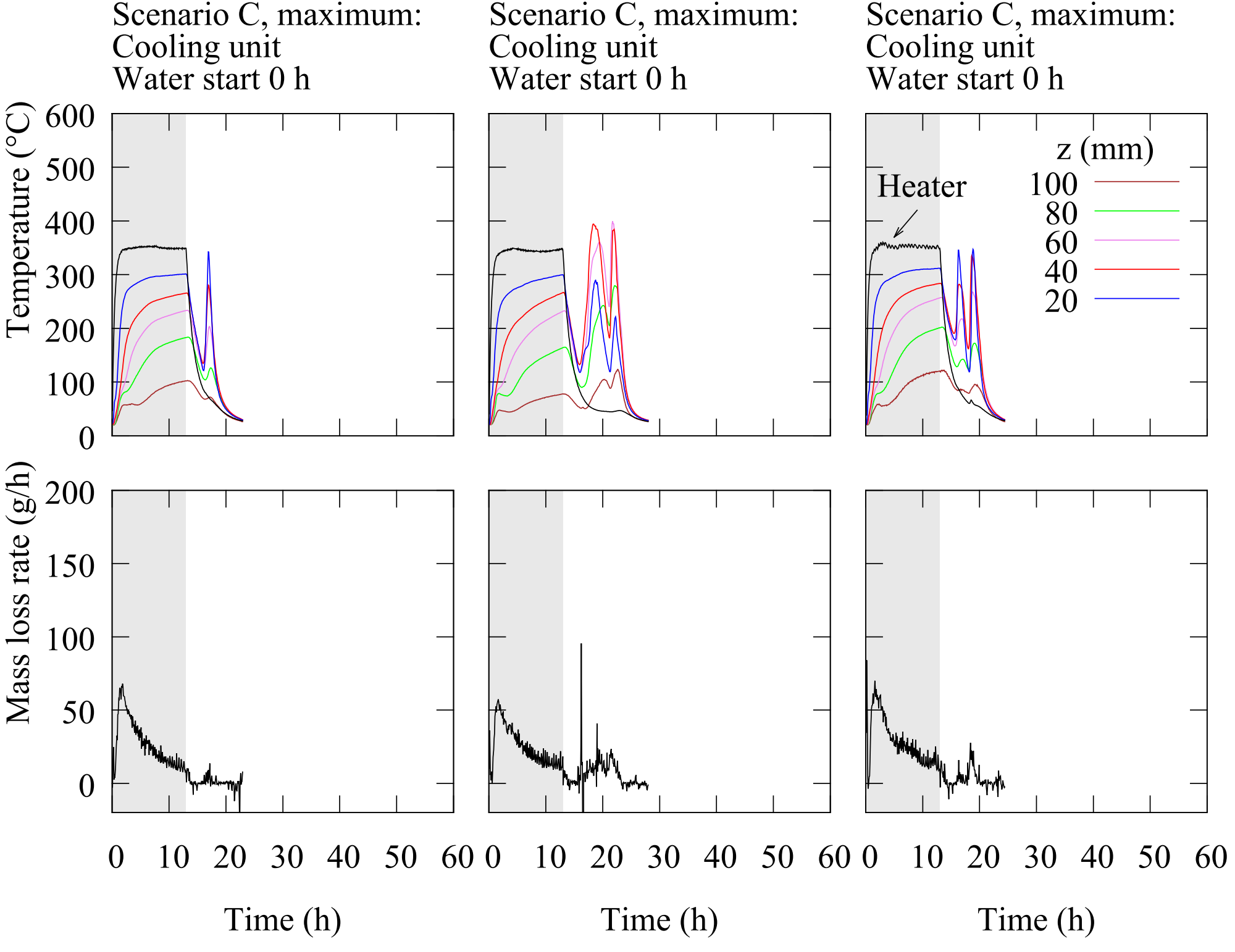
Scenario C, maximum:
Cooling unit
Water start 0 h
Scenario C, maximum:
Cooling unit
Water start 0 h
Scenario C, maximum:
Cooling unit
Water start 0 h
Temperature (°C)
600
500
400
300
200
100
0
z (mm)
Heater
100
80
60
40
20
Mass loss rate (g/h)
200
150
100
50
0
0 10 20 30 40 50 60
0 10 20 30 40 50 60
0 10 20 30 40 50 60
Time (h)
Time (h)
Time (h)

Fig8

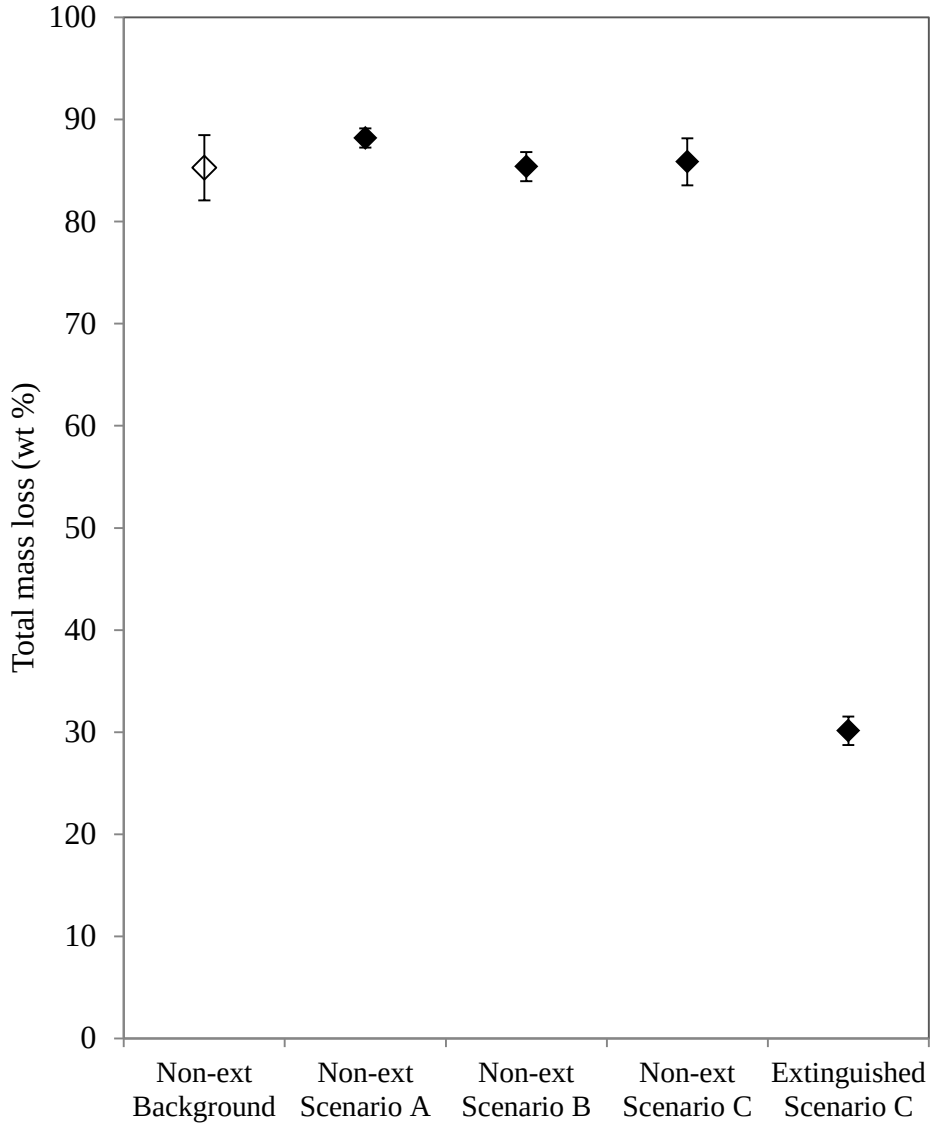
Total mass loss (wt %)
100
90
80
70
60
50
40
30
20
10
0
Non-ext Background
Non-ext Scenario A
Non-ext Scenario B
Non-ext Scenario C
Extinguished Scenario C

(a)

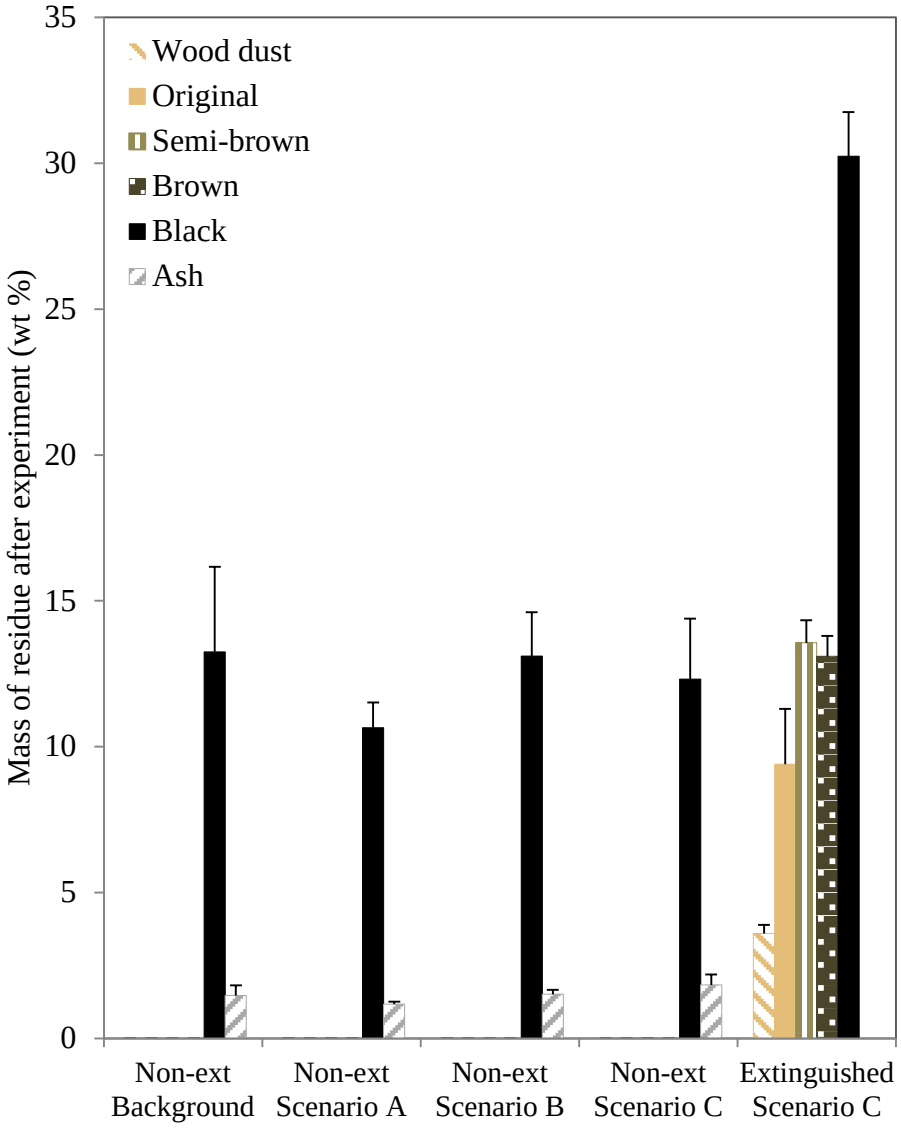
Mass of residue after experiment (wt %)
35
30
25
20
15
10
5
0
Wood dust
Original
Semi-brown
Brown
Black
Ash
Non-ext Background
Non-ext Scenario A
Non-ext Scenario B
Non-ext Scenario C
Extinguished Scenario C

(b)

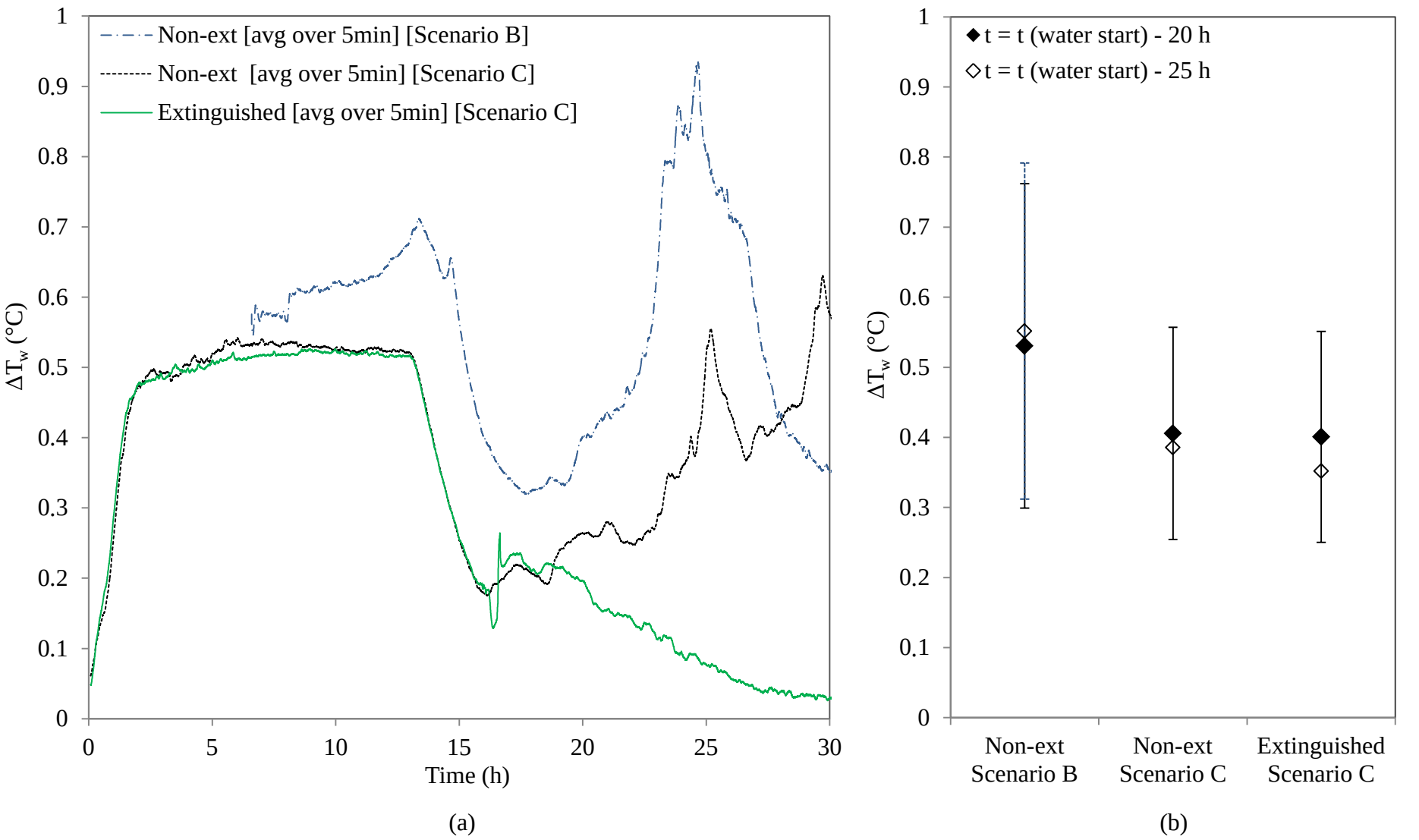
Non-ext [avg over 5min] [Scenario B]
Non-ext [avg over 5min] [Scenario C]
Extinguished [avg over 5min] [Scenario C]
ΔTw (°C)
Time (h)
0
0.1
0.2
0.3
0.4
0.5
0.6
0.7
0.8
0.9
1
0
5
10
15
20
25
30
(a)
t = t (water start) - 20 h
t = t (water start) - 25 h
ΔTw (°C)
Non-ext Scenario B
Non-ext Scenario C
Extinguished Scenario C
(b)

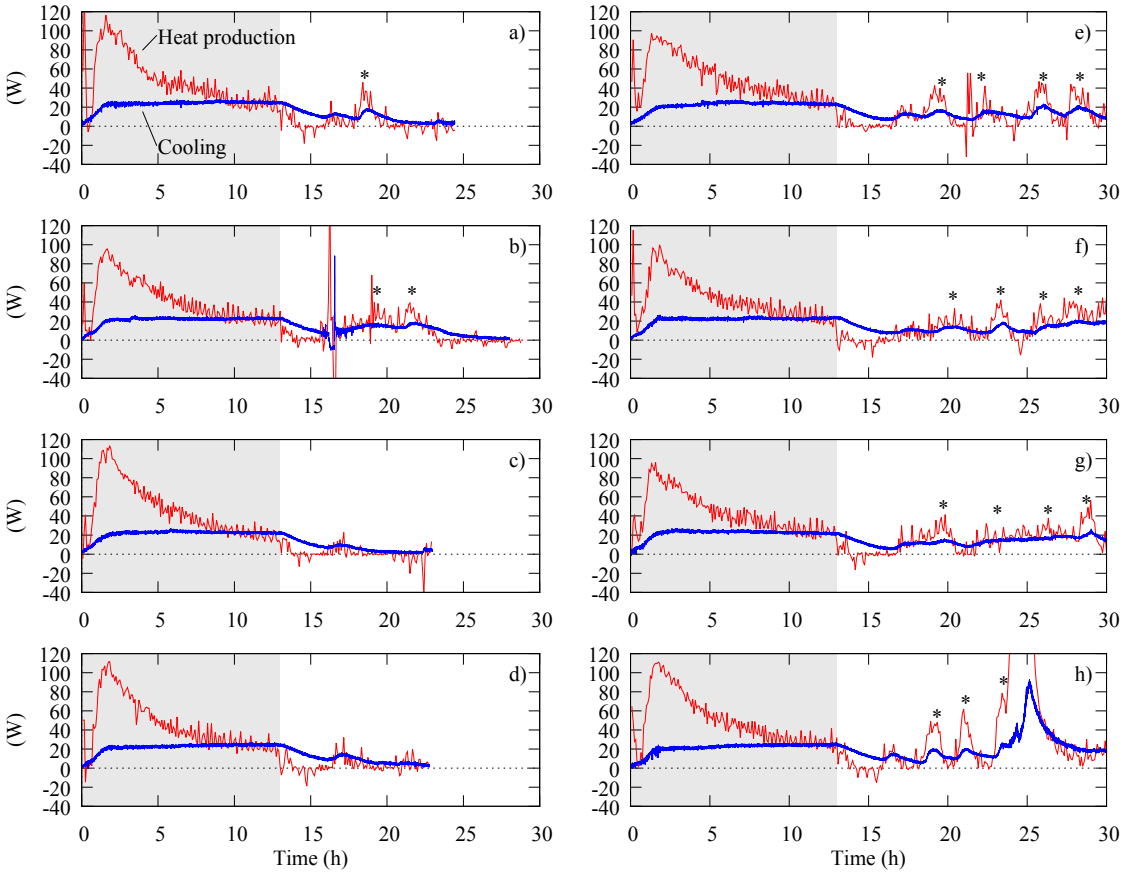
Heat production
Cooling
(W)
Time (h)
a)
b)
c)
d)
e)
f)
g)
h)
Extinguished, scenario C
Non-extinguished, scenario C

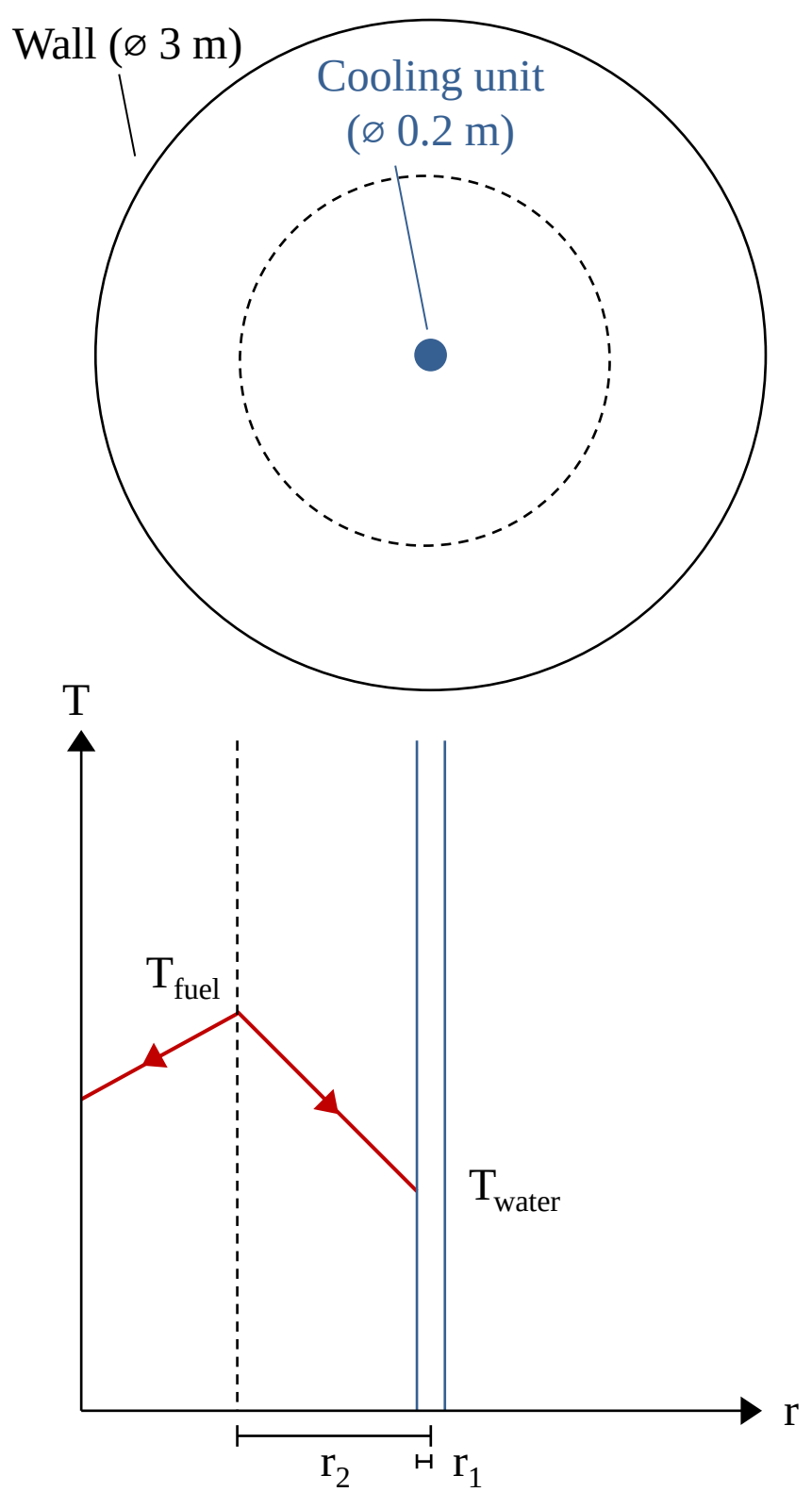
Wall (⌀ 3 m)
Cooling unit
(⌀ 0.2 m)
T
T fuel
T water
r
r2
r1